

See discussions, stats, and author profiles for this publication at: <https://www.researchgate.net/publication/257309044>

# Thiazolopyridine Ureas as Novel Antitubercular Agents Acting Through Inhibition of DNA Gyrase B.

ARTICLE in JOURNAL OF MEDICINAL CHEMISTRY · OCTOBER 2013

Impact Factor: 5.45 · DOI: 10.1021/jm401268f · Source: PubMed

CITATIONS

23

READS

79

## 34 AUTHORS, INCLUDING:



**Prakash Vachaspati**

7 PUBLICATIONS 55 CITATIONS

SEE PROFILE



**Jitendar Reddy**

AstraZeneca

18 PUBLICATIONS 133 CITATIONS

SEE PROFILE



**Giri Gaonkar**

Theralndx Lifesciences

12 PUBLICATIONS 670 CITATIONS

SEE PROFILE



**Julie A Tucker**

Newcastle University

28 PUBLICATIONS 1,097 CITATIONS

SEE PROFILE

# Thiazolopyridine Ureas as Novel Antitubercular Agents Acting through Inhibition of DNA Gyrase B

Manoj G. Kale,<sup>†</sup> Anandkumar Raichurkar,<sup>†,∇</sup> Shahul Hameed P,<sup>†,∇</sup> David Waterson,<sup>†,○</sup> David McKinney,<sup>||</sup> M. R. Manjunatha,<sup>†</sup> Usha Kranthi,<sup>†</sup> Krishna Koushik,<sup>†</sup> Lalit kumar Jena,<sup>†</sup> Vikas Shinde,<sup>†</sup> Suresh Rudrapatna,<sup>†</sup> Shubhada Barde,<sup>†</sup> Vaishali Humnabadkar,<sup>‡</sup> Prashanti Madhavapeddi,<sup>‡</sup> Halesha Basavarajappa,<sup>‡</sup> Anirban Ghosh,<sup>‡</sup> VK. Ramya,<sup>‡</sup> Supreeth Guptha,<sup>‡</sup> Sreevalli Sharma,<sup>‡</sup> Prakash Vachaspati,<sup>§,◆</sup> K.N. Mahesh Kumar,<sup>§,||</sup> Jayashree Giridhar,<sup>§,■</sup> Jitendar Reddy,<sup>§</sup> Vijender Panduga,<sup>§</sup> Samit Ganguly,<sup>§</sup> Vijaykamal Ahuja,<sup>§</sup> Sheshagiri Gaonkar,<sup>§,☆</sup> C. N. Naveen Kumar,<sup>§</sup> Derek Ogg,<sup>⊥</sup> Julie A. Tucker,<sup>⊥,□</sup> P. Ann Boriack-Sjodin,<sup>#,△</sup> Sunita M. de Sousa,<sup>‡</sup> Vasana K. Sambandamurthy,<sup>‡</sup> and Sandeep R. Ghorpade<sup>\*,†</sup>

<sup>†</sup>Department of Medicinal Chemistry, <sup>‡</sup>Department of Biosciences, and <sup>§</sup>DMPK and Animal Sciences, AstraZeneca India Pvt. Ltd., Bellary Road, Hebbal, Bangalore 560024, India

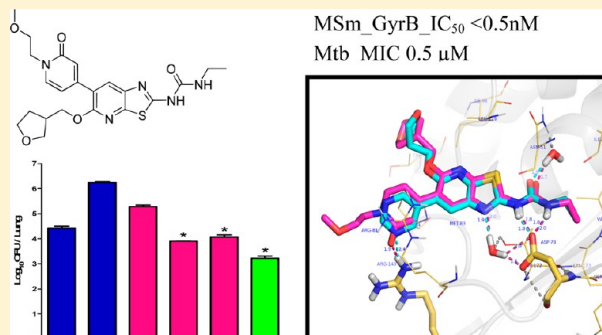
<sup>||</sup>Chemistry, Infection iMed, AstraZeneca, Waltham, Massachusetts 02451, United States

<sup>⊥</sup>Discovery Sciences, AstraZeneca, Alderley Park, Macclesfield SK10 4TF, United Kingdom

<sup>#</sup>Biosciences, Infection iMed, AstraZeneca, Waltham, Massachusetts 02451, United States

## **S** Supporting Information

**ABSTRACT:** A pharmacophore-based search led to the identification of thiazolopyridine ureas as a novel scaffold with antitubercular activity acting through inhibition of DNA Gyrase B (GyrB) ATPase. Evaluation of the binding mode of thiazolopyridines in a *Mycobacterium tuberculosis* (Mtb) GyrB homology model prompted exploration of the side chains at the thiazolopyridine ring C-5 position to access the ribose/solvent pocket. Potent compounds with GyrB IC<sub>50</sub> ≤ 1 nM and Mtb MIC ≤ 0.1 μM were obtained with certain combinations of side chains at the C-5 position and heterocycles at the C-6 position of the thiazolopyridine core. Substitutions at C-5 also enabled optimization of the physicochemical properties. Representative compounds were cocrystallized with *Streptococcus pneumoniae* (Spn) ParE; these confirmed the binding modes predicted by the homology model. The target link to GyrB was confirmed by genetic mapping of the mutations conferring resistance to thiazolopyridine ureas. The compounds are bactericidal in vitro and efficacious in vivo in an acute murine model of tuberculosis.



MSm\_GyrB\_IC<sub>50</sub> < 0.5 nM  
Mtb MIC 0.5 μM

## ■ INTRODUCTION

Tuberculosis (TB) continues to be a major cause of morbidity and mortality worldwide, claiming approximately three million lives each year.<sup>1</sup> The first-line TB drugs currently used are at least 40 years old, and the rapid emergence of drug-resistant strains of *Mycobacterium tuberculosis* (Mtb) is a major concern. Second-line drugs used for the treatment of multidrug resistant (MDR) and extensively drug resistant (XDR) TB have variable efficacy and induce serious side effects.<sup>2</sup> Hence, there is an urgent need to discover antitubercular agents with novel mechanisms of action to add to newer combination regimens for treating MDR- and XDR-TB.<sup>1,2</sup> Even though there are a few promising compounds in clinical development, such as bedaquiline,<sup>3</sup> delamanid,<sup>4</sup> SQ109,<sup>5</sup> oxazolidinones,<sup>6</sup> and fluoroquinolones,<sup>7</sup> the discovery of novel antimycobacterial agents

to replenish this emerging TB pipeline is critical.<sup>8</sup> The fluoroquinolones (FQ), as a class, have been found to be effective against drug-resistant TB. However, the emergence of resistance to FQs may prevent their effectiveness in the long term.<sup>9</sup> The Mtb genome is unique in encoding only two topoisomerases, topoisomerase I and DNA gyrase,<sup>10</sup> unlike the *Escherichia coli* genome, which encodes four topoisomerases.<sup>11</sup> Unlike other bacteria, Mtb does not have a type IV topoisomerase. The presence of a single type I topoisomerase and a single type II topoisomerase in Mtb is attractive from a drug-discovery perspective because it makes the enzyme more vulnerable to inhibition.

**Received:** August 18, 2013

**Published:** October 3, 2013

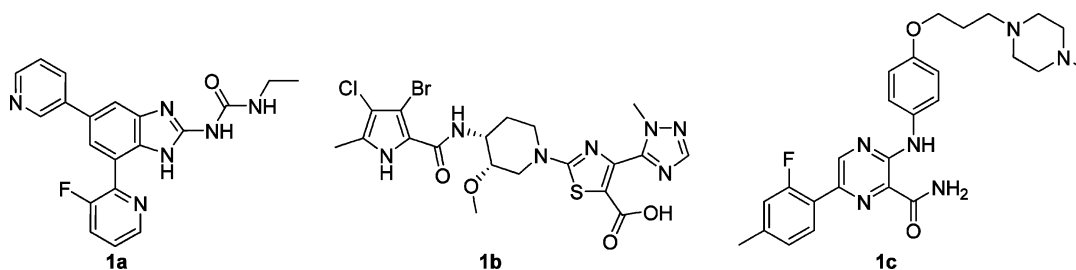


Figure 1. Known GyrB inhibitors with antitubercular activity.

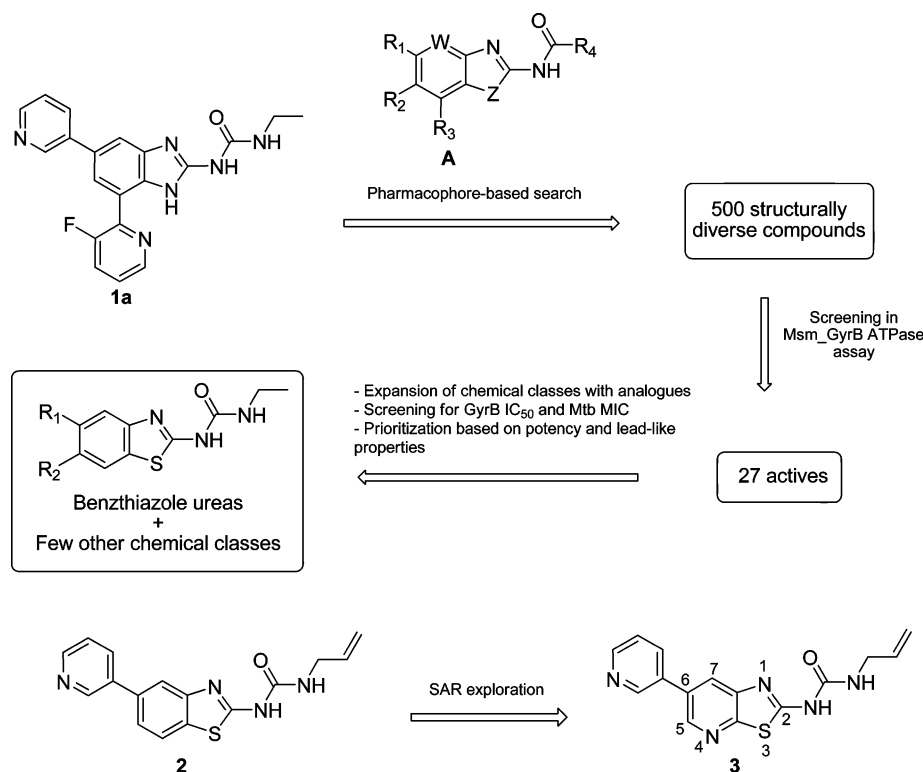


Figure 2. Scaffold hopping from benzimidazoles to thiazolopyridines.

FQs inhibit the activity of bacterial DNA gyrase by binding to the GyrA subunit and trapping the gyrase–DNA covalent complex, which induces oxidative damage and eventually leads to bacterial cell death.<sup>12</sup> Compounds like novobiocin and coumermycin inhibit the ATPase activity of the GyrB subunit of DNA gyrase, thereby depriving bacteria of the source of energy needed for maintaining the topological state of DNA in the cell and affecting processes such as DNA replication.<sup>13</sup> Developing novel inhibitors that target the GyrB subunit offers an excellent opportunity to address FQ resistance and to develop an effective treatment for TB.<sup>14</sup> Several GyrB inhibitors with antitubercular activity have been previously described, and these include the benzimidazole ureas<sup>15</sup> (1a) from Vertex and the pyrrolamides<sup>16</sup> (1b) and pyrazinamides<sup>17</sup> (1c) from AstraZeneca (Figure 1).

Benzimidazole ureas are active against FQ-resistant Mtb strains and are efficacious in murine models of TB.<sup>15a</sup> A few other aryl urea scaffolds are reported in the literature with moderate to potent antibacterial activity, such as triazolopyridine ureas,<sup>18</sup> benzthiazole ureas,<sup>19</sup> imidazolopyridine ureas,<sup>20</sup> and pyridine ureas.<sup>21</sup> All of these compounds act through dual inhibition of GyrB and ParE enzymes, but antitubercular properties of these compounds are not reported. Scaffold

hopping efforts using benzimidazole ureas as a starting point led to the identification of thiazolopyridine ureas as potent antitubercular agents acting through inhibition of GyrB ATPase activity.<sup>22</sup> This study describes the building of a structure–activity relationship of the thiazolopyridine ureas for the inhibition of GyrB ATPase, which resulted in the identification of a potent series suitable for lead optimization.

## RESULTS AND DISCUSSION

**Pharmacophore-Based Search.** A list of 500 diverse compounds from the AstraZeneca compound collection was identified on the basis of pharmacophore matching with the benzimidazole ureas (structure A, Figure 2). These compounds were tested for inhibition of *Mycobacterium smegmatis* (Msm) DNA GyrB ATPase;<sup>22</sup> the Msm enzyme was used instead of the Mtb enzyme because of the much higher specific activity of the Msm protein (manuscript in preparation). Among the small number of actives, the benzthiazole ureas (represented by compound 2, Figure 2) were identified as a promising chemical class with potent GyrB inhibition and a moderate MIC on Mtb. As part of general SAR exploration, it was observed that introduction of a nitrogen at the 4-position of the benzthiazole

core (compound 3, Figure 1) was well tolerated, leading to inhibition of GyrB and Mtb MIC that were similar to those seen with 2. This change also resulted in reduced logD and decreased plasma protein binding (Table 1). Hence, the structure–activity relationship of this thiazolopyridine scaffold for GyrB inhibition was explored utilizing structural information from an Mtb GyrB homology model.<sup>23</sup>

**Table 1. Comparison of Benzthiazole 2 with Thiazolopyridine 3**

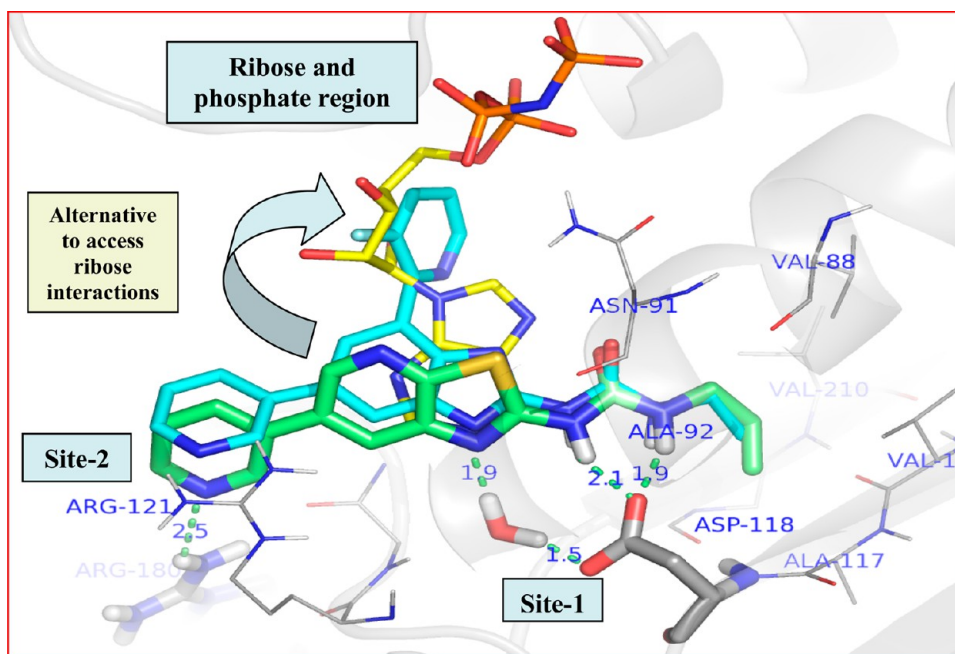
| properties                            | 2   | 3   |
|---------------------------------------|-----|-----|
| Msm_GyrB ATPase IC <sub>50</sub> (nM) | 160 | 88  |
| Mtb_MIC (μM)                          | 16  | 8   |
| logD pH <sub>7.4</sub>                | 3.9 | 2.9 |
| solubility pH <sub>7.4</sub> (μM)     | 7.5 | 6.5 |
| human PPB (% free)                    | 0.7 | 3.2 |

**Homology Modeling.** Docking of compounds 3 and 1a into an Mtb GyrB homology model suggested that the ligands occupied the ATP-binding site and had common interactions (Figure 3). Asp118 was involved in direct hydrogen-bond (HB) interactions with hydrogens of the two urea nitrogens and a water-mediated HB interaction with N1 of the thiazolopyridine ring; these are referred to as site-1 interactions. Arg121 lay above the 3-pyridyl ring, making cation  $\pi$ -stacking interactions, and Arg180 makes a HB interaction with the 3-pyridyl nitrogen atom; these are referred as site-2 interactions. In the case of the benzimidazole ureas, the pocket occupied by the ribose of ATP was accessed by the pyridine ring attached to the benzimidazole C-4 position.<sup>15b,c</sup> This interaction was considered important for the optimal binding of the ligand in the ATP-binding pocket of GyrB. However, in the case of thiazolopyridine urea 3, similar access to the ribose pocket is not possible because of the

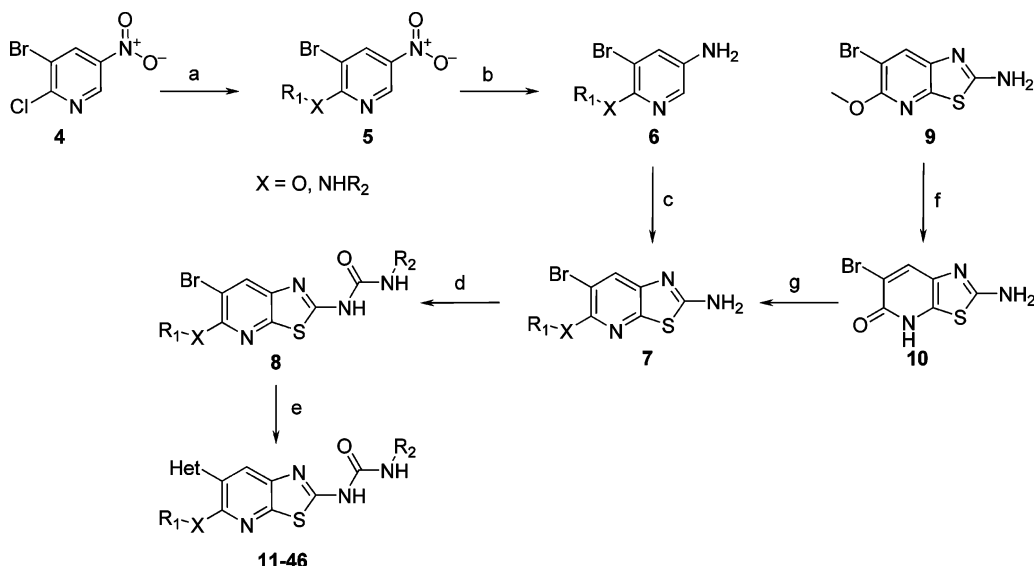
nitrogen at the thiazolopyridine 4-position. Hence, flexible side chains were added at the C-5 position (see Figure 2 for numbering) to extend into the ribose pocket with the aim of improving the potency of GyrB inhibition. These side chains may also serve as a chemical handle to modulate the physicochemical properties of the compounds.

**Chemistry.** The synthesis of thiazolopyridines with side chains at the C-5 position was achieved as shown in Scheme 1. Various side chains could be attached to the pyridine ring at the C-2 position to form intermediates of type 5 in good yield by reacting 3-bromo-2-chloro-5-nitropyridine (4) with an alcohol or amine in the presence of a base. Intermediate 5 was reduced using Zn/NH<sub>4</sub>Cl or Sn/HCl to synthesize aminopyridine 6. This was treated with potassium thiocyanate and bromine to produce the 2-aminothiazolopyridines, 7, in moderate yield. Alternatively, O-linked side chains could be introduced by the Mitsunobu reaction of thiazolopyridone amine 10 with the corresponding alcohols to obtain intermediates of type 7. Ethyl and allyl ureas 8 were formed in good yields by heating intermediate 7 with the corresponding isocyanate in the presence of triethylamine under microwave irradiation at 110 °C. Various heterocycles could be coupled to intermediate 8 under Suzuki conditions to yield the desired thiazolopyridine urea compounds 11–46 in moderate to good yields.

**Cocrystal Structures with *Streptococcus pneumoniae* (Spn) ParE.** Repeated attempts to obtain cocrystal structures of selected thiazolopyridine ureas with Mtb GyrB were unsuccessful. Given the high degree of conservation of the GyrB active site across bacterial species,<sup>24</sup> *S. pneumoniae* (Spn) ParE protein was employed as a surrogate for cocrystallization studies with representative compounds. (Refer to Figure 4a for a comparison of ATP-binding sites of mycobacterial GyrB and Spn ParE. A primary sequence alignment of Msm and Mtb GyrBs with Spn ParE is shown in the Supporting Information,



**Figure 3.** Docking of molecules into an homology model of the Mtb GyrB ATP-binding site. Hypothetical binding modes of ATP (yellow), benzimidazole urea 1a (cyan), and compound 3 (green). Important residues that participate in ligand interactions are Asp118, a conserved H<sub>2</sub>O molecule, Arg121, and Arg180. Access to the ribose binding region by 3 can be achieved from the thiazolopyridine C-5 position. Dotted green lines indicate HB interactions with the protein.

Scheme 1. General Synthesis of Thiazolopyridine Ureas<sup>a</sup>

<sup>a</sup>Reagents and conditions: (a) R<sub>1</sub>OH/R<sub>1</sub>NH<sub>2</sub>, Na<sub>2</sub>CO<sub>3</sub>, DMF; (b) Zn/NH<sub>4</sub>Cl or SnCl<sub>2</sub>, HCl; (c) KSCN, Br<sub>2</sub>, CH<sub>3</sub>CO<sub>2</sub>H; (d) R<sub>2</sub>-N=C=O, Et<sub>3</sub>N, DME/THF 1:1, microwave 110 °C, 20 min; (e) Het-B(OH)<sub>2</sub>, Pd(PPh<sub>3</sub>)<sub>4</sub> or PdCl<sub>2</sub>(PPh<sub>3</sub>)<sub>2</sub>, DME/water 3:1, 90 °C, 4–15 h or microwave 110 °C, 30 min; (f) 40% HBr in acetic acid, 120 °C, 1 h; and (g) DEAD or DIAD, PPh<sub>3</sub> on resin, R-OH, THF, 0 °C, 1 h.

Figure S1.) Cocrystal structures of compounds **11** and **20** (Table 2) in complex with Spn ParE were solved (PDB code 4mbc and 4mb9, respectively), and the binding modes are shown in Figure 4b. The urea, thiazolopyridine, and pyrimidine/pyridine rings in both structures were positioned to form similar hydrogen-bond interactions with the protein. Asp78 (equivalent to Asp118 in Mtb) was involved in a direct HB interaction with the hydrogens of the urea nitrogen atoms and in a water-molecule-mediated HB interaction with N1 of the thiazolopyridine ring. The urea carbonyl formed an additional water-mediated HB interaction with the side chain of Asn51 (equivalent to Asn91 in Mtb). The terminal allyl carbon of **11** was closely positioned alongside the backbone carbonyl oxygen of Thr172. Substitution of ethyl for allyl, as in **20**, allowed the core to penetrate deeper into the active-site pocket, leading to tighter binding. This may explain the improved potencies for ethyl urea derivatives, in general, compared to the allyl urea derivatives (Table 2). The Arg81 side chain is positioned above the 3-pyridyl/5-pyrimidyl rings to make cation  $\pi$ -stacking interactions. The ring pyridine/pyrimidine nitrogens are positioned for HB interactions with the side chain of Arg140. The second pyrimidine ring nitrogen of **20** makes an additional HB interaction with a water molecule that is absent from the structure with **11**. In both the compounds, the alkoxy substituents extended out to the solvent, making no apparent interactions with the protein.

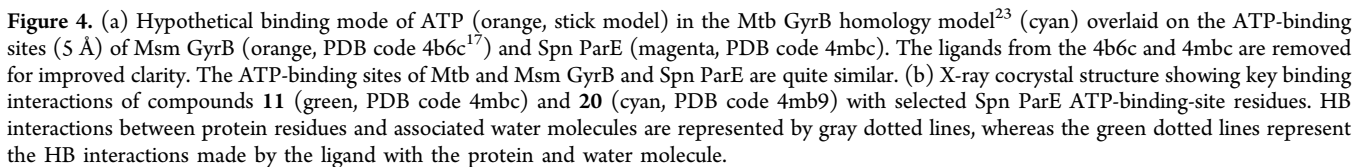
**SAR of O-Linked Side Chains at C-5.** Initially, the ribose-pocket interactions were explored by extending basic functionalities via an ethoxy linker from the C-5 position. Unfortunately, most of these compounds, represented by compound **11** (Table 2) with a morpholinylethoxy side chain, had less potent GyrB IC<sub>50</sub>'s compared to the parent compound **3** and had no effect on Mtb growth at the highest concentration tested. However, addition of neutral side chains like 2-methoxyethoxy at the C-5 position (Table 2, compound **12**) improved GyrB IC<sub>50</sub>'s and Mtb MICs. Changing the allyl urea to ethyl urea led to a marginal improvement in GyrB IC<sub>50</sub> and a nearly 4-fold improvement in Mtb MIC (Table 2, compare

compounds **12** and **13**). Hence, ethyl urea was chosen over allyl urea for further explorations. Branched side chain and cyclic ether side chains yielded compounds with improved inhibition of GyrB as well as lower Mtb MICs (Table 2, compounds **14–18**). The influence of the stereochemistry of the side chains on enzyme potency and Mtb MIC was minimal because these side chains are oriented toward the solvent-exposed region of the active site (Table 1, compounds **17** and **18**). Replacement of pyridine with pyrimidine at C-6 resulted in a 4–10-fold improvement in Mtb MICs without a significant change in GyrB inhibition (Table 1, compare compounds **13** and **15** with compounds **19** and **20**, respectively). This suggests improved permeation of pyrimidine-containing compounds across the Mtb cell wall.

The chemical space at the C-7 position of the thiazolopyridine ring was explored by the addition of a methyl group (compound **21**), but this led to a deterioration of GyrB inhibition and no inhibition of Mtb growth at the highest concentration tested. The lower potency for **21** may be attributed to the narrow and hydrophilic nature of the binding region around C-7 of the thiazolopyridine ring, leading to a clash of the C-7 methyl with the enzyme (see Figure S2 in the Supporting Information for the docked pose of compound **21** in Spn ParE).

**N-Linked Side Chains at C-5.** A series of side chains were introduced on the thiazolopyridine ureas via a nitrogen-atom linker at the C-5 position (Table 3). Most of the compounds with primary amine NH-linked substituents (R<sub>2</sub> = H) were slightly less potent inhibitors of GyrB and had higher Mtb MICs compared to analogues with O-linked side chains. However, the NH linker offered the advantage of better physicochemical properties (e.g., better aqueous solubility and excellent free plasma concentration), probably as a consequence of lower logD values (Table 3). The use of secondary amines for the N-linker led to a deterioration of the potency (compounds **25** and **26**). This may be due to a steric clash between the hydrophobic N-R<sub>2</sub> and hydrophilic residues that fold over the thiazolopyridine core (see Figure S3 in the





**Optimization of Heterocycle at Site-2.** On the basis of the binding-mode information, interactions of the heterocycle

Table 2. SAR of O-Linked Side Chains at the C-5 Position

| Compound  | R1 | R2    | Het           | Msm_GyrB<br>IC <sub>50</sub> (nM) | Mtb_MIC<br>(μM) |
|-----------|----|-------|---------------|-----------------------------------|-----------------|
| <b>11</b> |    | Allyl | 3-pyridyl     | 400                               | >50             |
| <b>12</b> |    | Allyl | 3-pyridyl     | 46                                | 10              |
| <b>13</b> |    | Ethyl | 3-pyridyl     | 25                                | 2.8             |
| <b>14</b> |    | Ethyl | 3-pyridyl     | 12                                | 1.29            |
| <b>15</b> |    | Ethyl | 3-pyridyl     | 5                                 | 1.3             |
| <b>16</b> |    | Ethyl | 3-pyridyl     | 9                                 | 0.92            |
| <b>17</b> |    | Ethyl | 3-pyridyl     | 13                                | 1.54            |
| <b>18</b> |    | Ethyl | 3-pyridyl     | 39                                | 0.92            |
| <b>19</b> |    | Ethyl | 5-pyrimidinyl | 17                                | 0.67            |
| <b>20</b> |    | Ethyl | 5-pyrimidinyl | 10                                | 0.2             |
| <b>21</b> |    |       |               | 1400                              | >20             |

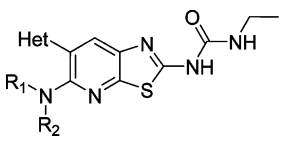
at the thiazolopyridine C-6 position with arginines in site-2 of the GyrB active-site pocket were hypothesized to be critical for potent GyrB inhibition. Hence, substitutions on these heterocycles were expected to impact GyrB inhibition. In addition, there is the potential to extend flexible substituents from the site-2 heterocycle into solvent, which may help in modulating physicochemical properties. Substituents like F, CH<sub>3</sub>, OCH<sub>3</sub>, and CN on the pyridine/pyrimidine ring at the thiazolopyridine C-6 position resulted in equipotent compounds with decreased aqueous solubility and lower free-plasma fractions (Table 4, compounds 27–34). Addition of a solubilizing 2-dimethylaminoethoxy substituent on the pyridine ring resulted in highly soluble compounds (solubility >1 mM) with potent GyrB IC<sub>50</sub>'s but poor to modest Mtb MICs (Table 4, compounds 35 and 36). Interestingly, addition of a morpholinylethoxy substituent on the pyridine ring resulted in compound 37 (Table 4) with a more potent Mtb MIC (1 μM) and high solubility. This might indicate better permeation of morpholinyl derivative 37 across the Mtb cell wall because of the reduced basicity (predicted pK<sub>a</sub> ~7.0) compared to the dimethylaminoethoxy analogues (predicted pK<sub>a</sub> ~9.0).

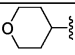
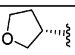
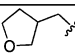
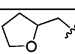
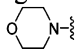
A small number of other heterocycles were introduced at the thiazolopyridine C-6 position for structural diversity with the aim of further optimization of the potency and physicochemical properties. A five-member pyrazole ring at this position resulted in compound 38 with potent GyrB inhibition and Mtb MIC comparable to the pyridine derivatives (Table 4, compare with

15 in Table 2). Interestingly, *N*-methylpyridone at site-2 (position-6 of the thiazolopyridine ring) improved Msm GyrB inhibition potency, with an IC<sub>50</sub> of 1 nM and Mtb MIC of 0.14 μM for compound 39 (Table 4, compare with 15 and 20 in Table 2). The pyridone ring could be substituted at C-6 with hydrophobic groups like methyl and isopropyl while retaining the potency of GyrB inhibition and Mtb MIC (Table 4, compounds 40 and 41). The pyridone N could be substituted with solubilizing neutral and basic substituents, leading to potent compounds with improved aqueous solubility (Table 4, compounds 42–46). Thus, the pyridone at site-2 provided a useful structural handle to modulate the physicochemical properties.

Docking of the most potent analogue, 42, into the Spn ParE crystal structure (Figure 5) showed that the distance between the carbonyl group of the pyridone ring and the guanidinium hydrogen of Arg140 is 1.9 Å. This is significantly shorter than the distance observed between the pyrimidine nitrogen of 20 and the guanidinium hydrogen of Arg140 (2.4 Å) in the Spn ParE–20 cocrystal structure. The closer proximity of the pyridone carbonyl to Arg140 may lead to a stronger HB interaction, accounting for the improvement in the enzyme-inhibitory potency. The methoxyethyl substituent is exposed to solvent and does not make any contact with protein residues in the docked pose (Figure 7). The reason that the methoxyethyl substituent has an improved GyrB IC<sub>50</sub> versus the *N*-methyl analogue (39) is not clear.

Table 3. SAR and Properties of Compounds with N-Linked Side Chains at the C-5 Position



| Compound | R1  | R2              | Het           | Msm_GyrB<br>IC <sub>50</sub> (nM) | Mtb<br>MIC<br>(μM) | LogD <sub>pH7.4</sub> <sup>a</sup> | Hu_PPB<br>(% free) <sup>a</sup> | Solubility<br>pH <sub>7.4</sub><br>(μM) <sup>a</sup> |
|----------|---|-----------------|---------------|-----------------------------------|--------------------|------------------------------------|---------------------------------|--|
| 22       |                            | H               | 3-pyridyl     | 30                                | 2                  | 2.53<br>(3.21)                     | 20 (5)                          | 634 (0.5)  |
| 23       |                            | H               | 3-pyridyl     | 30                                | 1                  | 2.0<br>(2.3)                       | 28 (5)                          | 152 (8)  |
| 24       |                            | H               | 3-pyridyl     | 90                                | 3.5                | 2.7<br>(2.8)                       | 40 (5)                          | 5000 (15)  |
| 25       |                            | CH <sub>3</sub> | 5-pyrimidinyl | 1100                              | >20                | ND <sup>b</sup>                    | ND <sup>b</sup>                 | ND <sup>b</sup>                                      |
| 26       | R1 and R2<br>together:<br> |                 | 5-pyrimidinyl | 500                               | >20                | ND <sup>b</sup>                    | ND <sup>b</sup>                 | ND <sup>b</sup>                                      |

<sup>a</sup>Values in parentheses are for the corresponding analogues with O-linked side chains at the C-5 position. <sup>b</sup>Not determined.

**MIC Correlation with GyrB IC<sub>50</sub>.** A plot of Msm GyrB pIC<sub>50</sub> (−log<sub>10</sub> of IC<sub>50</sub> in molar units) against Mtb pMIC (−log<sub>10</sub> of MIC in molar units) indicates a strong correlation between GyrB inhibition and Mtb MIC (Figure 6). In general, GyrB IC<sub>50</sub>'s below 100 nM (pIC<sub>50</sub> > 7) were required to attain Mtb MICs below 1 μM (pMIC > 6).

**Target Linkage by Spontaneous Resistance and Mutation Mapping.** The frequency of spontaneous resistance was determined by plating wild-type Mtb H37Rv on agar plates containing 2, 4, 8, or 16 μg/mL of **20**, concentrations corresponding to 8, 16, 32, or 64 times, respectively, the MIC of the compound. Spontaneous mutants arose at a frequency of approximately 3.1 × 10<sup>−8</sup>. No resistant mutants were obtained at 8 μg/mL or higher, indicating that this is the mutant-prevention concentration. The mutants demonstrated an 8–16-fold increase in MIC compared to the parent H37Rv strain for five analogues tested (data for two of the mutants are shown in Table 5). The strains resistant to compound **20** retained their MICs against isoniazid, rifampicin, and moxifloxacin, indicating specificity of the resistance mechanism.

Sequencing of the *gyrB* gene from the six spontaneous resistant strains to compound **20** revealed a single nucleotide change in the *gyrB* gene, resulting in an amino acid substitution at position 92 from alanine to serine (Ala92Ser), which is located in the GyrB ATP-binding domain. The Ala92Ser mutation on GyrB is in close vicinity to the Arg180His and Gly157Ser mutations that are reported to confer resistance to novobiocin and aminopyrazinamides, respectively, in Mtb.<sup>15a,17</sup> The mapping of resistance to thiazolopyridine ureas to *gyrB* establishes a strong target link of the Mtb MICs to GyrB inhibition. The Ala92Ser mutation also conferred resistance to the benzimidazole ureas.<sup>15a</sup>

To gain further insights into the observed mutation, an Mtb GyrB Ala92Ser mutant homology model was developed. The proposed binding mode of **20** in this homology model is shown in Figure 7a. Ala92 forms part of the site-1 region of the active site, providing a hydrophobic environment favorable to binding of the terminal ethyl of the urea group. Mutation of Ala92 to Ser introduces a hydroxyl group that not only generates a less favorable hydrophilic environment for the ethyl group but likely also affects the architecture of the pocket. In the mutant model, a new HB interaction was observed between the hydroxyl group of Ser92 and the carboxylate of Asp118. Comparison of the modeled binding modes of **20** in the WT and mutant GyrB suggests that the compound could retain some of the generic interactions in the mutant active site but there would also be some differences. For example, the compound had slightly shifted toward site-2 such that only one of the hydrogen atoms attached to the nitrogen of the urea is capable of making a HB interaction with Asp118. In addition, the thiazolopyridine rather than the pyrimidine now makes a cation  $\pi$ -interaction with Arg121. These changes may lead to suboptimal binding of **20** to the mutant, thus accounting for the higher MIC.

**Bactericidal Activity of Thiazolopyridine Ureas.** The thiazolopyridine ureas were highly bactericidal against replicating Mtb cells under in vitro conditions. The minimum bactericidal concentration (minimum concentration of drug that produces 2-logs units of killing in 7 days compared to the initial inoculum) of **23** was within 2-fold of the MIC for this series. A detailed time-kill experiment for a representative compound, **23**, revealed that the bactericidal activity under aerobic conditions is dependent on both time and drug concentration. The extent of the killing reached ~2.5 logs in 14 days at a drug concentration 16 times the MIC (Figure 8).

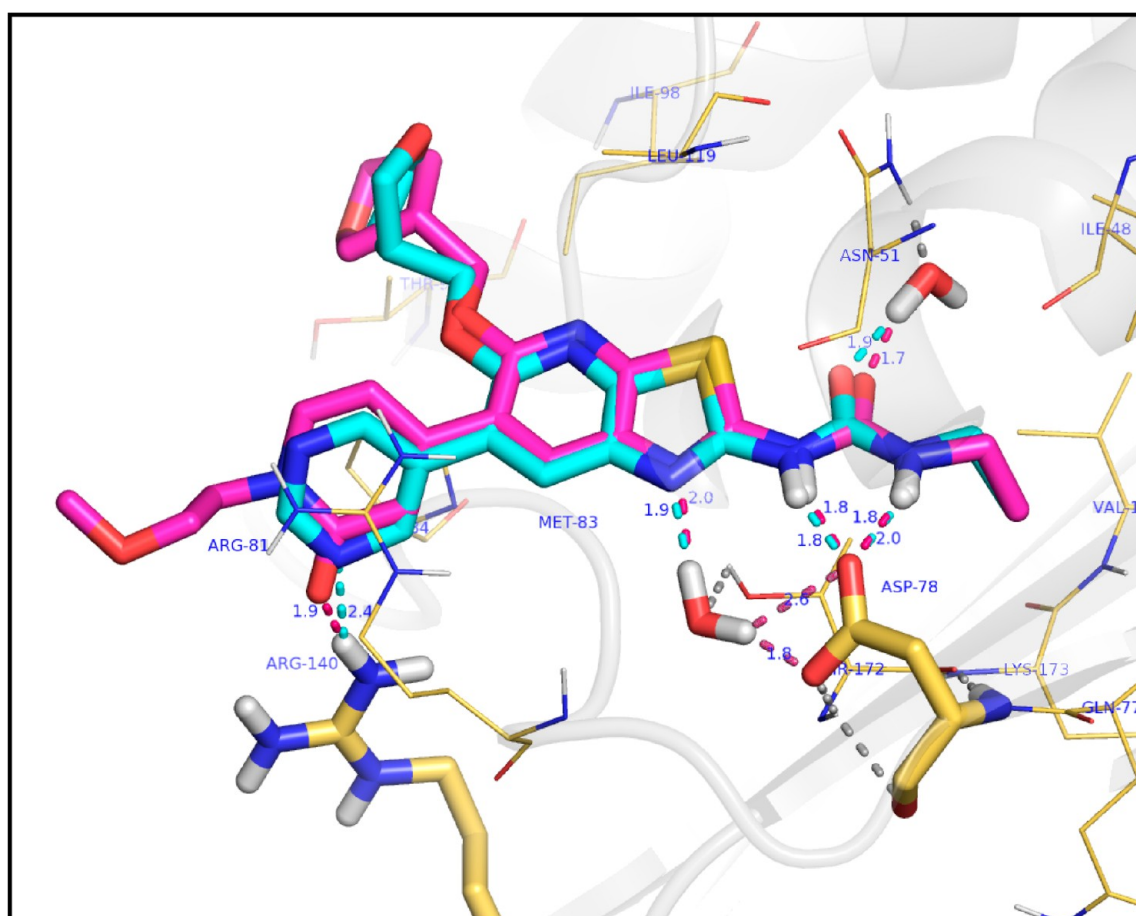


Table 4. SAR and Properties of Compounds with Heterocyclic Substitution in Site-2

| Compound | R1 | X  | Het | Msm_GyrB<br>IC <sub>50</sub> (nM) | Mtb_MIC<br>(μM) | Hu_PPB<br>% free | Aqueous<br>solubility<br>pH <sub>7.4</sub> (μM) |
|----------|----|----|-----|-----------------------------------|-----------------|------------------|---|
| 27       |    | O  |     | 9                                 | 0.9             | 0.6              | 3.7   |
| 28       |    | O  |     | 7                                 | 0.9             | 4                | 2   |
| 29       |    | O  |     | 11                                | 2               | 0.9              | 0.8   |
| 30       |    | O  |     | 8                                 | 1.7             | 2.5              | <0.5  |
| 31       |    | O  |     | 7                                 | 0.8             | 6                | <3  |
| 32       |    | O  |     | 14                                | 0.4             | ND <sup>a</sup>  | <1  |
| 33       |    | O  |     | 12                                | 0.6             | ND <sup>a</sup>  | <1  |
| 34       |    | NH |     | 47                                | 5               | 6                | 35  |
| 35       |    | O  |     | 14                                | >16             | ND <sup>a</sup>  | 2374  |
| 36       |    | O  |     | 10                                | 4               | 11               | >4000   |
| 37       |    | O  |     | 4                                 | 1               | 10               | 1386  |
| 38       |    | O  |     | 10                                | 1.8             | ND <sup>a</sup>  | 5   |
| 39       |    | O  |     | 1                                 | 0.14            | 5                | 6   |
| 40       |    | O  |     | 4.6                               | 0.14            | 8                | 5   |
| 41       |    | O  |     | 8                                 | 0.53            | 4                | 23  |
| 42       |    | O  |     | <0.5                              | 0.06            | 7                | ND <sup>a</sup>                                 |

Table 4. continued

| Compound | R1 | X  | Het | Msm_GyrB<br>IC <sub>50</sub> (nM) | Mtb_MIC<br>(μM) | Hu_PPB<br>% free | Aqueous<br>solubility<br>pH <sub>7.4</sub> (μM) |
|----------|----|----|-----|-----------------------------------|-----------------|------------------|---|
| 43       |    | O  |     | 2.5                               | 0.13            | 11               | 121   |
| 44       |    | NH |     | 3.7                               | 0.27            | 13               | 724   |
| 45       |    | O  |     | 3                                 | 3.1             | 5                | 5127  |
| 46       |    | O  |     | 2.2                               | 0.6             | 5                | 6118  |

<sup>a</sup>Not determined.

**Figure 5.** Pose of compound 42 (pink stick model) docked into the Spn ParE crystal structure overlaid with compound 20 (cyan) bound in the Spn ParE cocrystal (yellow, PDB code 4mb9).

**In Vivo Efficacy.** Having established the bactericidal activity of thiazolopyridine ureas against Mtb grown under in vitro conditions, the efficacy of these compounds was explored in an acute murine model of TB.<sup>25</sup> The efficacy results for compound

23 with good plasma exposure in mice following oral dosing (infected AUC = 200 μg hr/mL, fAUC/MIC = 100 at day 9 of dosing) are shown in Figure 9. Infected mice were treated with compound 23 for 10 days at three doses. A dose-dependent

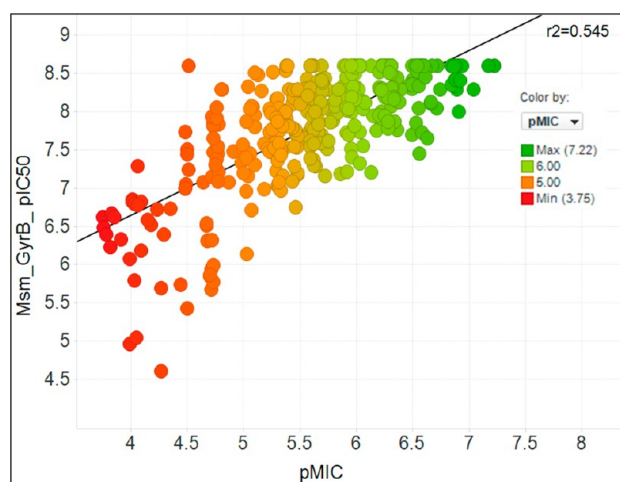


**Figure 6.** Scatter plot of Msm GyrB  $pIC_{50}$  vs Mtb  $pMIC$ ;  $pIC_{50} = -\log_{10}(IC_{50})$  and  $pMIC = -\log_{10}(MIC)$ , where  $IC_{50}$  and  $MIC$  are in molar units.

**Table 5.** MIC Modulation and Cross Resistance Exhibited by Resistant Mutants to Compound 20

| compound      | wild-type H37Rv | 20-resistant mutant clone 8.1 | 20-resistant mutant clone 8.2 |
|---------------|-----------------|-------------------------------|-------------------------------|
| 20            | 0.25            | 4                             | 4                             |
| 23            | 1               | 16                            | >16                           |
| 22            | 2               | 8                             | >16                           |
| 44            | 0.5             | 2                             | 2                             |
| 43            | 0.125           | 8                             | 16                            |
| isoniazid     | 0.015           | 0.015                         | 0.007                         |
| rifampicin    | 0.015           | 0.03                          | 0.06                          |
| mutation site | A92             | A92S                          | A92S                          |

effect on bacterial count in the lungs of mice was observed at the end of the treatment period (Figure 9). A 2-log kill in comparison to untreated controls was observed in the lungs of mice treated with compound 23 at doses of 300 mg/kg once daily (QD) or 150 mg/kg twice daily (BID) following 10 days of dosing. These two doses were bactericidal [i.e., CFU/lung was lower than in the early control, and the CFU/lung for both doses are statistically different from the early control ( $p < 0.05$ )], but the result of the two doses are not statistically different from one another.

The in vivo bactericidal activity observed provides evidence that in vivo target engagement of thiazolopyridines with Mtb GyrB results in enhanced efficacy in an acute murine model of TB.

## CONCLUSIONS

The thiazolopyridine ureas are potent antitubercular agents acting through the inhibition of DNA GyrB ATPase activity. These compounds are efficacious in a murine model of tuberculosis. The series has excellent lead-like properties and has structural handles for further optimization of pharmacokinetic properties. These compounds have the potential to treat drug-susceptible as well as drug-resistant TB, including quinolone-resistant TB, because they target a different activity of DNA gyrase. Preliminary studies, focusing primarily on the MIC and enzyme inhibition, have been presented here. The in vivo efficacy validates GyrB ATPase as a suitable target for the development of antitubercular agents. Although these results are very promising, lead optimization is needed to build in

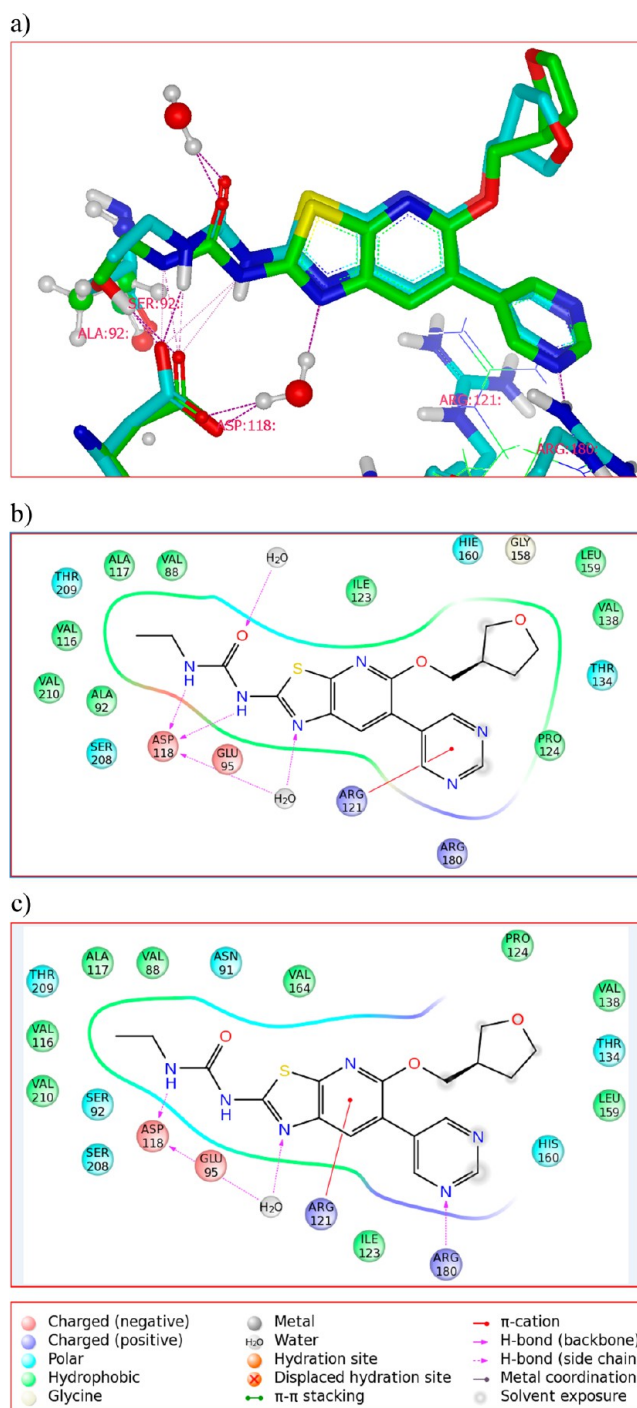


**Figure 7.** (a) Modeled binding mode of compound 20 in wild-type (green) and the A92S mutant (cyan) homology models of Mtb GyrB. Two-dimensional interaction plots of compound 20 in (b) WT and (c) A92S Mtb GyrB homology models.

pharmacokinetic properties and an adequate safety profile and to ensure that the dose to man would be in an acceptable range to enable progression of this series into clinical development to treat both drug-susceptible as well as drug-resistant TB.

## EXPERIMENTAL SECTION

**Chemistry.** All commercial reagents and solvents were used without further purification. Analytical thin-layer chromatography (TLC) was performed on  $SiO_2$  plates on alumina. Visualization was accomplished by UV irradiation at 254 and 220 nm. Flash column

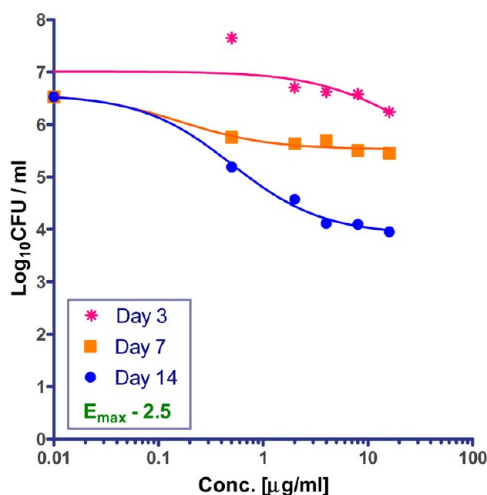


Figure 8. Kinetics of Mtb killing in broth exhibited by compound 23.

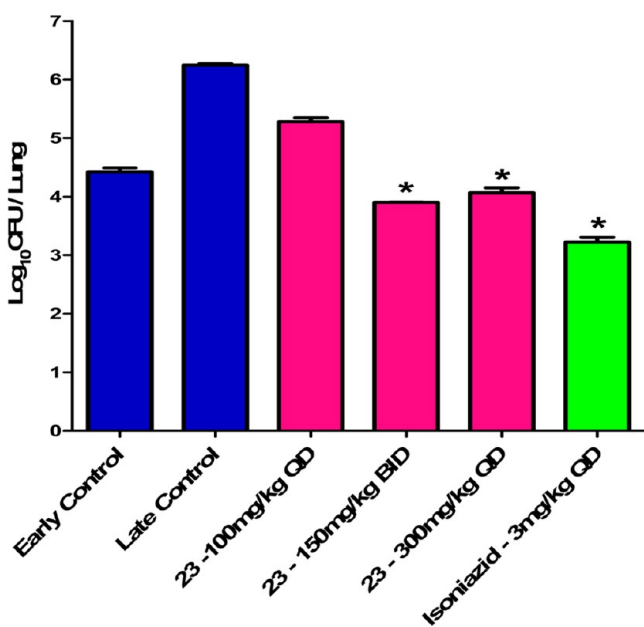


Figure 9. Efficacy of compound 23 in an acute murine model of tuberculosis. Balb/c mice were infected with Mtb H37Rv via the aerosol route to result in ~10 000 CFU/lung. Treatment was initiated 3 days postinfection, and varying doses of compounds were administered via oral gavage for 10 days. Mice ( $n = 3$ ) were sacrificed at the end of treatment, and the lung homogenates were plated to enumerate the bacterial counts. Isoniazid administered at 3 mg/kg served as a positive control. Asterisk (\*) denotes statistical significance with  $p < 0.05$ ; the CFU in the 150 mg/kg BID dose is not significantly different from that of the 300 mg/kg QD dose.

chromatography was performed using the Biotage Isolera flash purification system with SiO<sub>2</sub> 60 (particle size 0.040–0.055 mm, 230–400 mesh). The purity of all final derivatives for biological testing was confirmed to be >95%, as determined using the following conditions: a Shimadzu HPLC instrument with a Hamilton reversed-phase column (HxSil, C18, 3 μm, 2.1 mm × 50 mm (H2)). Eluent A, 5% CH<sub>3</sub>CN in H<sub>2</sub>O; eluent B, 90% CH<sub>3</sub>CN in H<sub>2</sub>O. A flow rate of 0.2 mL/min was used with UV detection at 254 and 214 nm. The structure of the intermediates and end products was confirmed by <sup>1</sup>H NMR and mass spectroscopy. Proton magnetic resonance spectra were determined in DMSO-*d*<sub>6</sub> unless otherwise stated using Bruker DRX-300 or Bruker DRX-400 spectrometers operating at 300 or 400 MHz, respectively. Splitting patterns are indicated as follows: s, singlet; d,

doublet; t, triplet; m, multiplet; br, broad peak. LCMS data was acquired using Agilent LCMS VL series. Source: ES ionization coupled with an Agilent 1100 series HPLC system and an Agilent 1100 series PDA as the front end. HRMS data was acquired using an Agilent 6520, quadrupole time-of-flight tandem mass spectrometer (Q-TOF MS/MS) coupled with an Agilent 1200 series HPLC system.

**General Procedure for Suzuki Coupling of Intermediate 8 with Corresponding Boronic Acids.** In a microwave vial, intermediate 8 (0.33 mmol), arylboronic acid or boronate (83 mg, 0.67 mmol), and sodium bicarbonate (56.0 mg, 0.67 mmol) were mixed with DME (8 mL) and water (2 mL). The mixture was purged with N<sub>2</sub> for 10 min. Pd(PPh<sub>3</sub>)<sub>4</sub> (57.7 mg, 0.05 mmol) was added to the mixture, and the mixture was microwaved for 80 min at 115 °C. The reaction mixture was cooled to rt and concentrated under vacuum. The residue was diluted with water (10 mL) and extracted with dichloromethane (thrice). The organic layers were combined, dried over sodium sulfate, and concentrated under vacuum. The residue was purified by flash chromatography on a silica gel column using MeOH-DCM as the eluent. Pure fractions were combined and evaporated under vacuum to obtain the pure final compound as crystalline material in 40–80% yield.

**1-Allyl-3-[6-(3-pyridyl)thiazolo[5,4-b]pyridin-2-yl]urea (3).** Yield: 39%. <sup>1</sup>H NMR (300 MHz, DMSO-*d*<sub>6</sub>) δ 3.85 (t,  $J = 7.0$  Hz, 2H), 5.13–5.30 (m, 2H), 5.85–5.90 (m, 1H), 6.97 (t,  $J = 5.0$  Hz, 1H), 7.50–7.60 (m, 1H), 8.20 (m, 1H), 8.33 (s, 1H), 8.65 (m, 1H), 8.75 (s, 1H), 9.00 (s, 1H), 11.00 (br, 1H). HRMS:  $m/z$  (ES+) 312.0911 (MH<sup>+</sup>) for C<sub>15</sub>H<sub>13</sub>N<sub>5</sub>O<sub>2</sub>S.

**1-[5-(2-Morpholin-4-ylethoxy)-6-pyridin-3-yl][1,3]thiazolo[5,4-b]pyridin-2-yl]-3-prop-2-en-1-ylurea (11).** Yield: 30%. <sup>1</sup>H NMR (300 MHz, DMSO-*d*<sub>6</sub>) δ 1.30–1.50 (m, 5H), 2.35–2.45 (m, 3H), 2.65 (t,  $J = 6.0$  Hz, 2H), 3.80 (t,  $J = 6.0$  Hz, 2H), 4.45 (t,  $J = 6.0$  Hz, 2H), 5.10 (d,  $J = 9.0$  Hz, 1H), 5.20 (d,  $J = 18.0$  Hz, 1H), 5.82–5.98 (m, 1H), 6.88 (t,  $J = 5.0$  Hz, 1H), 7.41–7.49 (m, 1H), 8.04 (s, 1H), 8.05–8.11 (m, 1H), 8.55 (d,  $J = 1.5$  Hz, 1H), 8.88 (s, 1H), 10.75 (br, 1H). HRMS:  $m/z$  (ES+) 441.1711 (MH<sup>+</sup>) for C<sub>21</sub>H<sub>24</sub>N<sub>6</sub>O<sub>3</sub>S.

**1-Allyl-3-[5-(2-methoxyethoxy)-6-pyridin-3-yl][1,3]thiazolo[5,4-b]pyridin-2-yl]urea (12).** Yield: 60%. <sup>1</sup>H NMR (300 MHz, DMSO-*d*<sub>6</sub>) δ 3.40 (s, 3H), 3.65 (t,  $J = 6.0$  Hz, 2H), 3.85 (t,  $J = 6.0$  Hz, 2H), 4.45 (t,  $J = 6.0$  Hz, 2H), 5.10 (d,  $J = 9.0$  Hz, 1H), 5.20 (d,  $J = 18.0$  Hz, 1H), 5.82–5.98 (m, 1H), 6.88 (t,  $J = 5.0$  Hz, 1H), 7.41–7.49 (m, 1H), 8.04 (s, 1H), 8.05–8.11 (m, 1H), 8.55 (d,  $J = 1.5$  Hz, 1H), 8.88 (s, 1H), 10.75 (br, 1H). HRMS:  $m/z$  (ES+) 386.1294 (MH<sup>+</sup>) for C<sub>18</sub>H<sub>19</sub>N<sub>5</sub>O<sub>3</sub>S.

**1-Ethyl-3-[5-(2-methoxyethoxy)-6-pyridin-3-yl][1,3]thiazolo[5,4-b]pyridin-2-yl]urea (13).** Yield: 52%. <sup>1</sup>H NMR (300 MHz, DMSO-*d*<sub>6</sub>) δ 1.10 (t,  $J = 7.1$  Hz, 3H), 3.12–3.23 (m, 2H), 3.30 (s, 3H), 3.68 (t,  $J = 4.5$  Hz, 2H), 4.50 (t,  $J = 4.5$  Hz, 2H), 6.68 (t,  $J = 5.4$  Hz, 1H), 7.45–7.50 (dd,  $J = 8.0, 4.9$  Hz, 1H), 8.03 (s, 1H), 8.06 (t,  $J = 2.5$  Hz, 1H), 8.55 (d,  $J = 4.8$  Hz, 1H), 8.82 (s, 1H), 10.70 (br, 1H). HRMS:  $m/z$  (ES+) 373.1214 (MH<sup>+</sup>) for C<sub>17</sub>H<sub>19</sub>N<sub>5</sub>O<sub>3</sub>S.

**(S)-1-Ethyl-3-[5-(1-methoxypropan-2-yloxy)-6-(pyridin-3-yl)thiazolo[5,4-b]pyridin-2-yl]urea (14).** Yield: 50%. <sup>1</sup>H NMR (400 MHz, DMSO-*d*<sub>6</sub>) δ 1.10 (t,  $J = 7.3$  Hz, 3H), 1.28 (d,  $J = 6.0$  Hz, 3H), 3.19 (quin,  $J = 6.8$  Hz, 2H), 3.26 (s, 3H), 3.46–3.56 (m, 2H), 5.35–5.53 (m, 1H), 6.70 (br s, 1H), 7.48 (dd,  $J = 7.5, 5.0$  Hz, 1H), 7.97–8.21 (m, 2H), 8.56 (d,  $J = 4.5$  Hz, 1H), 8.83 (s, 1H), 10.74 (br, 1H). HRMS:  $m/z$  (ES+) 388.1434 (MH<sup>+</sup>) for C<sub>18</sub>H<sub>21</sub>N<sub>5</sub>O<sub>3</sub>S.

**1-Ethyl-3-[6-pyridin-3-yl-5-(tetrahydrofuran-3-ylmethoxy)[1,3]thiazolo[5,4-b]pyridin-2-yl]urea (15).** Yield: 65%. <sup>1</sup>H NMR (300 MHz, DMSO-*d*<sub>6</sub>) δ 1.10 (t,  $J = 7.1$  Hz, 3H), 1.60–1.70 (m, 1H), 1.90–2.02 (m, 1H), 2.55–2.65 (m, 1H), 3.13–3.23 (m, 2H), 3.50 (dd,  $J = 6.0, 6.0$  Hz, 1H), 3.65–3.75 (m, 3H), 4.25–4.40 (m, 2H), 6.68 (t,  $J = 10.0$  Hz, 1H), 7.45–7.50 (m, 1H), 7.95–8.04 (m, 1H), 8.05 (s, 1H), 8.55 (d,  $J = 2.5$  Hz, 1H), 8.80 (s, 1H), 10.70 (br, 1H). HRMS:  $m/z$  (ES+) 400.1439 (MH<sup>+</sup>) for C<sub>19</sub>H<sub>21</sub>N<sub>5</sub>O<sub>3</sub>S.

**1-Ethyl-3-[6-(pyridin-3-yl)-5-(tetrahydro-2H-pyran-4-yloxy)thiazolo[5,4-b]pyridin-2-yl]urea (16).** Yield: 50%. <sup>1</sup>H NMR (400 MHz, DMSO-*d*<sub>6</sub>) δ 1.09 (t,  $J = 7.2$  Hz, 3H), 1.61–1.65 (m, 2H), 1.95–2.05 (m, 2H), 3.11–3.25 (m, 2H), 3.50–3.60 (m, 2H), 3.70–3.80 (m, 2H), 5.25–5.39 (m, 1H), 6.69 (t,  $J = 4.9$  Hz, 1H), 7.48–



7.51 (m, 1H), 8.04–8.07 (m, 2H), 8.56–8.57 (dd,  $J = 3.0$ , 1H), 8.82–8.83 (d,  $J = 2.5$  Hz, 1H), 10.75 (br, 1H). HRMS:  $m/z$  (ES<sup>+</sup>) 400.1428 (MH<sup>+</sup>) for C<sub>19</sub>H<sub>21</sub>N<sub>5</sub>O<sub>3</sub>S.

(R)-1-Ethyl-3-(6-(pyridin-3-yl)-5-(tetrahydrofuran-3-yloxy)-thiazolo[5,4-b]pyridin-2-yl)urea (**17**). Yield: 40%. <sup>1</sup>H NMR (400 MHz, DMSO-*d*<sub>6</sub>)  $\delta$  1.10 (t,  $J = 7.0$  Hz, 3H), 2.00 (m, 1H), 2.2–2.31 (m, 1H), 3.14–3.24 (m, 2H), 3.73–3.82 (m, 3H), 3.94 (dd,  $J = 10.5$ , 4.5 Hz, 1H), 5.65 (t,  $J = 5.3$  Hz, 1H), 6.70 (t,  $J = 5.0$  Hz, 1H), 7.50 (m, 1H), 8.05 (m, 2H), 8.55 (d,  $J = 2.5$  Hz, 1H), 8.85 (s, 1H), 10.73 (br, 1H). HRMS:  $m/z$  (ES<sup>+</sup>) 386.1295 (MH<sup>+</sup>) for C<sub>18</sub>H<sub>19</sub>N<sub>5</sub>O<sub>3</sub>S.

(S)-1-Ethyl-3-(6-(pyridin-3-yl)-5-(tetrahydrofuran-3-yloxy)-thiazolo[5,4-b]pyridin-2-yl)urea (**18**). Yield: 55%. <sup>1</sup>H NMR (DMSO-*d*<sub>6</sub>)  $\delta$  1.10 (t,  $J = 7.1$  Hz, 3H), 1.95–2.05 (m, 1H), 2.19–2.31 (m, 1H), 3.14–3.25 (m, 2H), 3.72–3.83 (m, 3H), 3.94 (dd,  $J = 10.3$ , 4.6 Hz, 1H), 5.64 (t,  $J = 5.36$  Hz, 1H), 6.70 (d,  $J = 5.04$  Hz, 1H), 7.49 (dd,  $J = 7.7$ , 4.89 Hz, 1H), 7.99–8.11 (m, 2H), 8.57 (d,  $J = 4.1$  Hz, 1H), 8.81 (s, 1H), 10.75 (br, 1H). HRMS:  $m/z$  (ES<sup>+</sup>) 386.1292 (MH<sup>+</sup>) for C<sub>18</sub>H<sub>19</sub>N<sub>5</sub>O<sub>3</sub>S.

1-Ethyl-3-[5-(2-methoxyethoxy)-6-pyrimidin-5-yl][1,3]thiazolo[5,4-b]pyridin-2-yl)urea (**19**). Yield: 52%. <sup>1</sup>H NMR (300 MHz, DMSO-*d*<sub>6</sub>)  $\delta$  1.10 (t,  $J = 7.1$  Hz, 3H), 3.13–3.24 (m, 2H), 3.30 (s, 3H), 3.68 (t,  $J = 4.5$  Hz, 2H), 4.50 (t,  $J = 4.5$  Hz, 2H), 6.68 (t,  $J = 5.5$  Hz, 1H), 8.20 (s, 1H), 9.10 (s, 2H), 9.18 (s, 1H), 10.75 (br, 1H). HRMS:  $m/z$  (ES<sup>+</sup>) 375.1233 (MH<sup>+</sup>) for C<sub>16</sub>H<sub>18</sub>N<sub>6</sub>O<sub>5</sub>S.

1-Ethyl-3-[6-pyrimidin-5-yl-5-(tetrahydrofuran-3-ylmethoxy)-[1,3]thiazolo[5,4-b]pyridin-2-yl)urea (**20**). Yield: 60%. <sup>1</sup>H NMR (300 MHz, DMSO-*d*<sub>6</sub>)  $\delta$  1.11 (t,  $J = 7.3$  Hz, 3H), 1.60–1.74 (m, 1H), 1.91–2.06 (m, 1H), 2.58–2.72 (m, 1H), 3.14–3.27 (m, 2H), 3.51 (dd,  $J = 8.6$ , 5.9 Hz, 1H), 3.59–3.79 (m, 3H), 4.25–4.42 (m, 2H), 6.67 (t,  $J = 5.7$  Hz, 1H), 8.17 (s, 1H), 9.03–9.09 (m, 2H), 9.17 (s, 1H), 10.65 (br, 1H). HRMS:  $m/z$  (ES<sup>+</sup>) 401.1382 (MH<sup>+</sup>) for C<sub>18</sub>H<sub>20</sub>N<sub>6</sub>O<sub>3</sub>S.

1-Ethyl-3-[7-methyl-6-(3-pyridyl)-5-[(3R)-tetrahydrofuran-3-yl]-oxy-thiazolo[5,4-b]pyridin-2-yl)urea (**21**). Yield: 30%. <sup>1</sup>H NMR (300 MHz, DMSO-*d*<sub>6</sub>)  $\delta$  1.10 (t,  $J = 7.1$  Hz, 3H), 1.75–1.91 (m, 2H), 2.07–2.21 (m, 1H), 2.31 (s, 3H), 3.15–3.24 (m, 2H), 3.54–3.73 (m, 3H), 3.88 (dd,  $J = 10.1$ , 4.7 Hz, 1H), 5.54 (t,  $J = 5.0$  Hz, 1H), 6.72 (t,  $J = 5.6$  Hz, 1H), 7.48 (dd,  $J = 7.6$ , 4.8 Hz, 1H), 7.75 (d,  $J = 7.9$  Hz, 1H), 8.50 (s, 1H), 8.57 (d,  $J = 4.7$  Hz, 1H), 10.70 (br, 1H). HRMS:  $m/z$  (ES<sup>+</sup>) 400.1444 (MH<sup>+</sup>) for C<sub>19</sub>H<sub>21</sub>N<sub>5</sub>O<sub>3</sub>S.

1-Ethyl-3-(6-(pyridin-3-yl)-5-(tetrahydro-2H-pyran-4-ylamino)-thiazolo[5,4-b]pyridin-2-yl)urea (**22**). Yield: 36%. <sup>1</sup>H NMR (400 MHz, DMSO-*d*<sub>6</sub>)  $\delta$  1.03–1.13 (m, 3H), 1.40–1.55 (m, 2H), 1.79–1.87 (m, 2H), 3.12–3.22 (m, 2H), 3.37–3.51 (m, 2H), 3.74–3.89 (m, 2H), 4.03–4.16 (m, 1H), 5.59 (d,  $J = 7.5$  Hz, 1H), 6.67 (t,  $J = 5.0$  Hz, 1H), 7.50 (dd,  $J = 7.5$ , 5.0 Hz, 1H), 7.56 (s, 1H), 7.90 (dt,  $J = 8.0$ , 2.0 Hz, 1H), 8.60 (dd,  $J = 5.0$ , 1.5 Hz, 1H), 8.66 (d,  $J = 1.5$  Hz, 1H), 10.45 (br, 1H). HRMS:  $m/z$  (ES<sup>+</sup>) 400.1428 (MH<sup>+</sup>) for C<sub>19</sub>H<sub>22</sub>N<sub>6</sub>O<sub>2</sub>S.

(S)-1-Ethyl-3-(6-(pyridin-3-yl)-5-(tetrahydrofuran-3-ylamino)-thiazolo[5,4-b]pyridin-2-yl)urea (**23**). Yield: 50%. <sup>1</sup>H NMR (400 MHz, DMSO-*d*<sub>6</sub>)  $\delta$  1.18 (t,  $J = 7.0$  Hz, 3H), 1.92 (m, 1H), 2.24 (m, 1H), 3.27 (m, 2H), 3.60 (dd,  $J = 8.8$ , 4.8 Hz, 1H), 3.71–3.82 (m, 1H), 3.82–3.93 (m, 1H), 4.00 (dd,  $J = 8.8$ , 6.3 Hz, 1H), 4.59 (m, 1H), 5.93 (d,  $J = 6.0$  Hz, 1H), 6.73 (br, 1H), 7.59 (dd,  $J = 8.0$ , 5.0 Hz, 1H), 7.67 (s, 1H), 7.88–7.90 (m, 1H), 8.69 (dd,  $J = 5.0$ , 1.5 Hz, 1H), 8.75 (d,  $J = 2.0$  Hz, 1H), 10.58 (br, 1H). HRMS:  $m/z$  (ES<sup>+</sup>) 385.1440 (MH<sup>+</sup>) for C<sub>18</sub>H<sub>20</sub>N<sub>6</sub>O<sub>2</sub>S.

1-Ethyl-3-(6-(pyridin-3-yl)-5-((tetrahydrofuran-3-yl)-methylamino)thiazolo[5,4-b]pyridin-2-yl)urea (**24**). Yield: 51%. <sup>1</sup>H NMR (300 MHz, DMSO-*d*<sub>6</sub>)  $\delta$  0.85 (t,  $J = 7.3$  Hz, 3H), 1.30–1.39 (m, 1H), 1.62–1.72 (m, 1H), 2.33–2.42 (m, 2H), 2.88–3.00 (m, 2H), 3.04 (t,  $J = 6.5$  Hz, 2H), 3.24 (dd,  $J = 8.5$ , 5.0 Hz, 1H), 3.31–3.54 (m, 2H), 5.82 (t,  $J = 5.5$  Hz, 1H), 6.55 (br, 1H), 7.17–7.34 (m, 2H), 7.59–7.68 (m, 1H), 8.30–8.45 (m, 2H), 10.35 (br, 1H). HRMS:  $m/z$  (ES<sup>+</sup>) 399.1600 (MH<sup>+</sup>) for C<sub>19</sub>H<sub>22</sub>N<sub>6</sub>O<sub>2</sub>S.

1-Ethyl-3-[5-[methyl(tetrahydrofuran-2-ylmethyl)amino]-6-pyrimidin-5-yl-thiazolo[5,4-b]pyridin-2-yl)urea (**25**). Yield: 45%. <sup>1</sup>H NMR (300 MHz, DMSO-*d*<sub>6</sub>)  $\delta$  1.10 (t,  $J = 7.2$  Hz, 3H), 1.23–1.41 (m, 1H), 1.66–1.86 (m, 3H), 2.65 (s, 3H), 3.09–3.25 (m, 4H), 3.50–3.71 (m, 2H), 3.86–3.98 (m, 1H), 6.67 (t,  $J = 5.6$  Hz, 1H), 7.89 (s, 1H), 9.01 (s, 2H), 9.15 (s, 1H), 10.58 (br, 1H). HRMS:  $m/z$  (ES<sup>+</sup>) 414.1714 (MH<sup>+</sup>) for C<sub>19</sub>H<sub>23</sub>N<sub>7</sub>O<sub>2</sub>S.

1-Ethyl-3-(5-morpholin-4-yl-6-pyrimidin-5-yl)[1,3]thiazolo[5,4-b]pyridin-2-yl)urea (**26**). Yield: 30%. <sup>1</sup>H NMR (300 MHz, DMSO-*d*<sub>6</sub>)  $\delta$  1.10 (t,  $J = 7.2$  Hz, 3H), 2.90–2.99 (m, 4H), 3.10–3.25 (m, 2H), 3.47–3.59 (m, 4H), 6.70 (t,  $J = 10.0$  Hz, 1H), 7.98 (s, 1H), 9.11–9.22 (m, 3H), 10.75 (br, 1H). HRMS:  $m/z$  (ES<sup>+</sup>) 386.1394 (MH<sup>+</sup>) for C<sub>17</sub>H<sub>19</sub>N<sub>7</sub>O<sub>2</sub>S.

1-Ethyl-3-[6-(6-fluoropyridin-3-yl)-5-(tetrahydrofuran-3-ylmethoxy)[1,3]thiazolo[5,4-b]pyridin-2-yl)urea (**27**). Yield: 59%. <sup>1</sup>H NMR (300 MHz, DMSO-*d*<sub>6</sub>)  $\delta$  1.10 (t,  $J = 7.1$  Hz, 3H), 1.60–1.70 (m, 1H), 1.90–2.02 (m, 1H), 2.55–2.65 (m, 1H), 3.13–3.23 (m, 2H), 3.50 (dd,  $J = 6.0$ , 6.0 Hz, 1H), 3.62–3.75 (m, 3H), 4.23–4.38 (m, 2H), 6.68 (t,  $J = 10.0$  Hz, 1H), 7.26–7.30 (m, 1H), 8.05 (s, 1H), 8.19–8.25 (m, 1H), 8.45 (s, 1H), 10.70 (br, 1H). HRMS:  $m/z$  (ES<sup>+</sup>) 418.1350 (MH<sup>+</sup>) for C<sub>19</sub>H<sub>20</sub>FN<sub>5</sub>O<sub>3</sub>S.

1-Ethyl-3-(6-(5-fluoropyridin-3-yl)-5-((tetrahydrofuran-3-yl)-methoxy)thiazolo[5,4-b]pyridin-2-yl)urea (**28**). Yield: 51%. <sup>1</sup>H NMR (300 MHz, DMSO-*d*<sub>6</sub>)  $\delta$  1.10 (t,  $J = 7.1$  Hz, 3H), 1.60–1.70 (m, 1H), 1.91–2.02 (m, 1H), 2.61–2.66 (m, 1H), 3.13–3.23 (m, 2H), 3.51 (dd,  $J = 6.0$ , 6.0 Hz, 1H), 3.62–3.75 (m, 3H), 4.22–4.37 (m, 2H), 6.67 (t,  $J = 10.0$  Hz, 1H), 7.97 (dd,  $J = 8.1$ , 2.5 Hz, 1H), 8.12 (s, 1H), 8.51 (d,  $J = 2.7$  Hz, 1H), 8.70 (s, 1H), 10.73 (br, 1H). HRMS:  $m/z$  (ES<sup>+</sup>) 418.1346 (MH<sup>+</sup>) for C<sub>19</sub>H<sub>20</sub>FN<sub>5</sub>O<sub>3</sub>S.

1-Ethyl-3-(6-(6-methylpyridin-3-yl)-5-((tetrahydrofuran-3-yl)-methoxy)thiazolo[5,4-b]pyridin-2-yl)urea (**29**). Yield: 68%. <sup>1</sup>H NMR (300 MHz, DMSO-*d*<sub>6</sub>)  $\delta$  1.09 (t,  $J = 7.2$  Hz, 3H), 1.66 (m, 1H), 1.89–2.05 (m, 1H), 2.52 (s, 3H), 2.55–2.70 (m, 1H), 3.12–3.26 (m, 2H), 3.50 (dd,  $J = 8.6$ , 5.9 Hz, 1H), 3.59–3.79 (m, 3H), 4.19–4.38 (m, 2H), 6.69 (t,  $J = 5.5$  Hz, 1H), 7.34 (d,  $J = 7.9$  Hz, 1H), 7.92 (dd,  $J = 8.0$ , 2.4 Hz, 1H), 8.02 (s, 1H), 8.66 (d,  $J = 2.3$  Hz, 1H), 10.74 (br, 1H). HRMS:  $m/z$  (ES<sup>+</sup>) 414.1597 (MH<sup>+</sup>) for C<sub>20</sub>H<sub>23</sub>N<sub>5</sub>O<sub>3</sub>S.

1-Ethyl-3-(6-(5-methoxypyridin-3-yl)-5-((tetrahydrofuran-3-yl)-methoxy)thiazolo[5,4-b]pyridin-2-yl)urea (**30**). Yield: 29%. <sup>1</sup>H NMR (300 MHz, DMSO-*d*<sub>6</sub>)  $\delta$  1.10 (t,  $J = 7.1$  Hz, 3H), 1.70–1.80 (m, 1H), 1.91–2.02 (m, 1H), 2.61–2.69 (m, 1H), 3.13–3.23 (m, 2H), 3.51 (dd,  $J = 6.0$ , 6.0 Hz, 1H), 3.62–3.75 (m, 3H), 3.89 (s, 3H), 4.27–4.34 (m, 2H), 6.93 (t,  $J = 10.0$  Hz, 1H), 7.61 (s, 1H), 8.03 (s, 1H), 8.27 (d,  $J = 2.7$  Hz, 1H), 8.39 (d,  $J = 3.0$  Hz, 1H), 11.00 (br, 1H). HRMS:  $m/z$  (ES<sup>+</sup>) 430.1542 (MH<sup>+</sup>) for C<sub>20</sub>H<sub>23</sub>N<sub>5</sub>O<sub>4</sub>S.

1-Ethyl-3-(6-(2-methylpyrimidin-5-yl)-5-((tetrahydrofuran-3-yl)-methoxy)thiazolo[5,4-b]pyridin-2-yl)urea (**31**). Yield: 25%. <sup>1</sup>H NMR (300 MHz, DMSO-*d*<sub>6</sub>)  $\delta$  1.10 (t,  $J = 7.3$  Hz, 3H), 1.58–1.77 (m, 1H), 1.89–2.08 (m, 1H), 2.68 (s, 4H), 3.12–3.26 (m, 2H), 3.43–3.58 (m, 1H), 3.58–3.84 (m, 3H), 4.18–4.44 (m, 2H), 6.69 (t,  $J = 5.4$  Hz, 1H), 8.15 (s, 1H), 8.94 (s, 2H), 10.72 (br, 1H). HRMS:  $m/z$  (ES<sup>+</sup>) 415.1601 (MH<sup>+</sup>) for C<sub>19</sub>H<sub>22</sub>N<sub>6</sub>O<sub>3</sub>S.

1-[6-(6-Cyanopyridin-3-yl)-5-(tetrahydrofuran-3-ylmethoxy)[1,3]thiazolo[5,4-b]pyridin-2-yl]-3-ethylurea (**32**). Yield: 45%. <sup>1</sup>H NMR (300 MHz, DMSO-*d*<sub>6</sub>)  $\delta$  1.10 (t,  $J = 7.1$  Hz, 3H), 1.60–1.70 (m, 1H), 1.90–2.02 (m, 1H), 2.55–2.65 (m, 1H), 3.13–3.23 (m, 2H), 3.50 (dd,  $J = 6.0$ , 6.0 Hz, 1H), 3.62–3.75 (m, 3H), 4.23–4.38 (m, 2H), 6.68 (t,  $J = 10.0$  Hz, 1H), 8.10–8.21 (m, 2H), 8.25–8.35 (m, 1H), 9.00 (s, 1H), 11.0 (br, 1H). HRMS:  $m/z$  (ES<sup>+</sup>) 425.1393 (MH<sup>+</sup>) for C<sub>20</sub>H<sub>20</sub>N<sub>6</sub>O<sub>3</sub>S.

1-[6-(5-Cyanopyridin-3-yl)-5-(tetrahydrofuran-3-ylmethoxy)[1,3]thiazolo[5,4-b]pyridin-2-yl]-3-ethylurea (**33**). Yield: 43%. <sup>1</sup>H NMR (300 MHz, DMSO-*d*<sub>6</sub>)  $\delta$  1.10 (t,  $J = 7.1$  Hz, 3H), 1.60–1.70 (m, 1H), 1.90–2.0 (m, 1H), 2.61–2.65 (m, 1H), 3.14–3.23 (m, 2H), 3.51 (dd,  $J = 6.0$ , 6.0 Hz, 1H), 3.59–3.75 (m, 3H), 4.24–4.39 (m, 2H), 6.72 (t,  $J = 10.0$  Hz, 1H), 8.16 (s, 1H), 8.55 (t,  $J = 4.2$  Hz, 1H), 9.0 (d,  $J = 2.7$  Hz, 1H), 9.1 (d,  $J = 3.0$  Hz, 1H), 10.8 (br, 1H). HRMS:  $m/z$  (ES<sup>+</sup>) 425.1395 (MH<sup>+</sup>) for C<sub>20</sub>H<sub>20</sub>N<sub>6</sub>O<sub>3</sub>S.

1-[6-(6-Cyanopyridin-3-yl)-5-(tetrahydro-2H-pyran-4-ylamino)-[1,3]thiazolo[5,4-b]pyridin-2-yl]-3-ethylurea (**34**). Yield: 20%. <sup>1</sup>H NMR (300 MHz, DMSO-*d*<sub>6</sub>)  $\delta$  1.1 (t,  $J = 7.2$  Hz, 3H), 1.40–1.56 (m, 2H), 1.83 (d,  $J = 9.8$  Hz, 2H), 3.10–3.23 (m, 2H), 3.42 (t,  $J = 10.6$  Hz, 2H), 3.84 (d,  $J = 11.1$  Hz, 2H), 4.11 (dd,  $J = 10.9$ , 3.6 Hz, 1H), 5.88 (d,  $J = 7.5$  Hz, 1H), 6.69 (t,  $J = 5.3$  Hz, 1H), 7.63 (s, 1H), 8.07–8.21 (m, 2H), 8.83 (s, 1H), 10.29 (br, 1H). HRMS:  $m/z$  (ES<sup>+</sup>) 424.1552 (MH<sup>+</sup>) for C<sub>20</sub>H<sub>21</sub>N<sub>7</sub>O<sub>2</sub>S.

1-[6-[6-(2-Dimethylamino)ethoxy]pyridin-3-yl]-5-(tetrahydrofuran-3-ylmethoxy)[1,3]thiazolo[5,4-b]pyridin-2-yl]-3-ethylurea (**35**). Yield: 54%. <sup>1</sup>H NMR (300 MHz, DMSO-*d*<sub>6</sub>)  $\delta$  1.10 (t,  $J = 7.1$  Hz,

3H), 1.65–1.72 (m, 1H), 1.91–2.02 (m, 1H), 2.20 (s, 6H), 2.63 (t,  $J = 5.7$  Hz, 3H), 3.13–3.23 (m, 2H), 3.51 (dd,  $J = 6.0, 6.0$  Hz, 1H), 3.62–3.77 (m, 3H), 4.23–4.40 (m, 4H), 6.75 (t,  $J = 10.0$  Hz, 1H), 6.86 (d,  $J = 9.0$  Hz, 1H), 7.92 (m, 2H), 8.35 (d,  $J = 2.4$  Hz, 1H), 10.8 (br, 1H). HRMS:  $m/z$  (ES<sup>+</sup>) 487.2119 (MH<sup>+</sup>) for C<sub>23</sub>H<sub>30</sub>N<sub>6</sub>O<sub>4</sub>S.

**1-[6-[5-[2-(Dimethylamino)ethoxy]pyridin-3-yl]-5-(tetrahydrofuran-3-ylmethoxy)[1,3]thiazolo[5,4-b]pyridin-2-yl]-3-ethylurea (36).** Yield: 25%. <sup>1</sup>H NMR (300 MHz, DMSO-*d*<sub>6</sub>)  $\delta$  1.10 (t,  $J = 7.1$  Hz, 3H), 1.65–1.72 (m, 1H), 1.91–2.02 (m, 1H), 2.23 (s, 6H), 2.67 (t,  $J = 6.0$  Hz, 3H), 3.19–3.25 (m, 2H), 3.50 (dd,  $J = 6.0, 6.0$  Hz, 1H), 3.59–3.79 (m, 3H), 4.19 (t,  $J = 5.7$  Hz, 2H), 4.21–4.39 (m, 2H), 6.70 (t,  $J = 10.0$  Hz, 1H), 7.62 (d,  $J = 0.9$  Hz, 1H), 8.05 (s, 1H), 8.27 (d,  $J = 3.4$  Hz, 1H), 8.39 (d,  $J = 1.8$  Hz, 1H), 10.70 (br, 1H). HRMS:  $m/z$  (ES<sup>+</sup>) 487.2121 (MH<sup>+</sup>) for C<sub>23</sub>H<sub>30</sub>N<sub>6</sub>O<sub>4</sub>S.

**1-Ethyl-3-[6-[5-(2-morpholin-4-ylethoxy)pyridin-3-yl]-5-(tetrahydrofuran-3-ylmethoxy)[1,3]thiazolo[5,4-b]pyridin-2-yl]urea (37).** Yield: 32%. <sup>1</sup>H NMR (300 MHz, DMSO-*d*<sub>6</sub>)  $\delta$  1.10 (t,  $J = 7.2$  Hz, 3H), 1.68 (dd,  $J = 12.6, 6.6$  Hz, 1H), 1.90–2.05 (m, 1H), 2.35–2.45 (m, 4H), 2.57–2.80 (m, 3H), 3.20 (qn,  $J = 6.7$  Hz, 2H), 3.47–3.80 (m, 8H), 4.18–4.42 (m, 4H), 6.69 (t,  $J = 5.3$  Hz, 1H), 7.64 (s, 1H), 8.07 (s, 1H), 8.28 (d,  $J = 2.5$  Hz, 1H), 8.40 (s, 1H), 10.70 (br, 1H). HRMS:  $m/z$  (ES<sup>+</sup>) 486.2056 (MH<sup>+</sup>) for C<sub>25</sub>H<sub>32</sub>N<sub>6</sub>O<sub>5</sub>S.

**1-Ethyl-3-[6-(1-methyl-1H-pyrazol-4-yl)-5-(tetrahydrofuran-3-ylmethoxy)[1,3]thiazolo[5,4-b]pyridin-2-yl]urea (38).** Yield: 40%. <sup>1</sup>H NMR (300 MHz, DMSO-*d*<sub>6</sub>)  $\delta$  1.09 (t,  $J = 7.1$  Hz, 3H), 1.65–1.79 (m, 1H), 2.0–2.1 (m, 1H), 2.75–2.90 (m, 1H), 3.12–3.22 (m, 2H), 3.55–3.75 (m, 2H), 3.80–3.88 (m, 2H), 3.89 (s, 3H), 4.25–4.39 (m, 2H), 6.66 (t,  $J = 10.0$  Hz, 1H), 8.02 (s, 1H), 8.16 (s, 1H), 8.21 (s, 1H), 10.70 (br, 1H). HRMS:  $m/z$  (ES<sup>+</sup>) 403.1545 (MH<sup>+</sup>) for C<sub>18</sub>H<sub>22</sub>N<sub>6</sub>O<sub>3</sub>S.

**1-Ethyl-3-[6-(1-methyl-2-oxo-1,2-dihydropyridin-4-yl)-5-((tetrahydrofuran-3-yl)methoxy)thiazolo[5,4-b]pyridin-2-yl]urea (39).** Yield: 40%. <sup>1</sup>H NMR (300 MHz, DMSO-*d*<sub>6</sub>)  $\delta$  1.09 (t,  $J = 7.2$  Hz, 3H), 1.60–1.70 (m, 1H), 1.90–2.05 (m, 1H), 2.60–2.70 (m, 1H), 3.10–3.33 (m, 2H), 3.45 (s, 3H), 3.50–3.60 (m, 1H), 3.65–3.85 (m, 3H), 4.20–4.40 (m, 2H), 6.47 (d,  $J = 5.1$  Hz, 1H), 6.61 (s, 1H), 6.69 (t,  $J = 10.0$  Hz, 1H), 7.70 (d,  $J = 6.0$  Hz, 1H), 7.99 (s, 1H), 10.72 (br, 1H). HRMS:  $m/z$  (ES<sup>+</sup>) 430.1543 (MH<sup>+</sup>) for C<sub>20</sub>H<sub>23</sub>N<sub>5</sub>O<sub>4</sub>S.

**1-[6-(1,6-Dimethyl-2-oxo-1,2-dihydropyridin-4-yl)-5-((tetrahydrofuran-3-yl)methoxy)thiazolo[5,4-b]pyridin-2-yl]-3-ethylurea (40).** Yield: 32%. <sup>1</sup>H NMR (300 MHz, DMSO-*d*<sub>6</sub>)  $\delta$  1.09 (t,  $J = 7.2$  Hz, 3H), 1.66–1.73 (m, 1H), 1.91–2.08 (m, 1H), 2.40 (s, 3H), 2.54–2.77 (m, 1H), 3.10–3.25 (m, 2H), 3.46 (s, 3H), 3.50–3.58 (m, 1H), 3.61–3.84 (m, 3H), 4.16–4.42 (m, 2H), 6.43 (s, 1H), 6.52 (s, 1H), 6.70 (s, 1H), 7.99 (s, 1H), 10.80 (br, 1H). HRMS:  $m/z$  (ES<sup>+</sup>) 444.1693 (MH<sup>+</sup>) for C<sub>21</sub>H<sub>25</sub>N<sub>5</sub>O<sub>4</sub>S.

**1-Ethyl-3-[6-(6-isopropyl-1-methyl-2-oxo-1,2-dihydropyridin-4-yl)-5-((tetrahydrofuran-3-yl)methoxy)thiazolo[5,4-b]pyridin-2-yl]urea (41).** Yield: 35%. <sup>1</sup>H NMR (300 MHz, DMSO-*d*<sub>6</sub>)  $\delta$  1.09 (t,  $J = 7.1$  Hz, 3H), 1.24 (d,  $J = 6.6$  Hz, 6H), 1.69–1.73 (m, 1H), 1.89–2.09 (m, 1H), 2.63–2.67 (m, 1H), 3.14–3.23 (m, 3H), 3.52–3.61 (m, 4H), 3.61–3.80 (m, 3H), 4.20–4.36 (m, 2H), 6.41 (s, 1H), 6.49 (s, 1H), 6.71 (br, 1H), 8.00 (s, 1H), 10.74 (br, 1H). HRMS:  $m/z$  (ES<sup>+</sup>) 472.2006 (MH<sup>+</sup>) for C<sub>23</sub>H<sub>29</sub>N<sub>5</sub>O<sub>4</sub>S.

**1-Ethyl-3-[6-(1-(2-methoxyethyl)-2-oxo-1,2-dihydropyridin-4-yl)-5-((tetrahydrofuran-3-yl)methoxy)thiazolo[5,4-b]pyridin-2-yl]urea (42).** Yield: 30%. <sup>1</sup>H NMR (300 MHz, DMSO-*d*<sub>6</sub>)  $\delta$  1.09 (t,  $J = 7.2$  Hz, 3H), 1.61–1.76 (m, 1H), 1.92–2.08 (m, 1H), 2.58–2.77 (m, 1H), 3.11–3.24 (m, 2H), 3.26 (s, 3H), 3.52 (dd,  $J = 8.7, 6.0$  Hz, 1H), 3.58–3.64 (m, 2H), 3.65–3.84 (m, 3H), 4.08 (t,  $J = 5.2$  Hz, 2H), 4.25 (dd,  $J = 10.4, 8.1$  Hz, 1H), 4.36 (dd,  $J = 10.5, 6.5$  Hz, 1H), 6.48 (dd,  $J = 7.1, 2.0$  Hz, 1H), 6.63 (d,  $J = 1.9$  Hz, 1H), 6.70 (t,  $J = 5.0$  Hz, 1H), 7.64 (d,  $J = 7.0$  Hz, 1H), 8.03 (s, 1H), 10.80 (br, 1H). HRMS:  $m/z$  (ES<sup>+</sup>) 474.1812 (MH<sup>+</sup>) for C<sub>22</sub>H<sub>27</sub>N<sub>5</sub>O<sub>5</sub>S.

**(R)-1-Ethyl-3-[6-(1-(2-methoxyethyl)-2-oxo-1,2-dihydropyridin-4-yl)-5-(tetrahydrofuran-3-yloxy)thiazolo[5,4-b]pyridin-2-yl]urea (43).** Yield: 36%. <sup>1</sup>H NMR (300 MHz, DMSO-*d*<sub>6</sub>)  $\delta$  1.10 (t,  $J = 7.2$  Hz, 3H), 1.97–2.10 (m, 1H), 2.19–2.34 (m, 1H), 3.13–3.24 (m, 2H), 3.27 (s, 3H), 3.62 (t,  $J = 5.4$  Hz, 2H), 3.75–3.89 (m, 3H), 3.91–4.00 (m, 1H), 4.08 (t,  $J = 5.3$  Hz, 2H), 5.60–5.69 (m, 1H), 6.48 (dd,  $J = 7.06, 2.0$  Hz, 1H), 6.63 (d,  $J = 1.9$  Hz, 1H), 6.69 (t,  $J = 5.8$  Hz, 1H),

7.62 (d,  $J = 7.2$  Hz, 1H), 8.02 (s, 1H), 10.73 (br, 1H). HRMS:  $m/z$  (ES<sup>+</sup>) 460.1656 (MH<sup>+</sup>) for C<sub>21</sub>H<sub>25</sub>N<sub>5</sub>O<sub>5</sub>S.

**(S)-1-Ethyl-3-[6-(1-(2-methoxyethyl)-2-oxo-1,2-dihydropyridin-4-yl)-5-(tetrahydrofuran-3-ylamino)thiazolo[5,4-b]pyridin-2-yl]urea (44).** Yield: 38%. <sup>1</sup>H NMR (300 MHz, DMSO-*d*<sub>6</sub>)  $\delta$  1.09 (t,  $J = 7.2$  Hz, 3H), 1.79–1.92 (m, 1H), 2.18 (dd,  $J = 12.2, 6.8$  Hz, 1H), 3.10–3.22 (m, 2H), 3.29 (br, 3H), 3.53 (dd,  $J = 8.7, 4.5$  Hz, 1H), 3.62 (t,  $J = 5.3$  Hz, 2H), 3.66–3.75 (m, 1H), 3.75–3.85 (m, 1H), 3.91 (dd,  $J = 8.9, 6.2$  Hz, 1H), 4.08 (t,  $J = 5.4$  Hz, 2H), 4.41–4.59 (m, 1H), 5.86 (d,  $J = 6.0$  Hz, 1H), 6.32 (dd,  $J = 7.1, 1.8$  Hz, 1H), 6.48 (s, 1H), 6.60–6.71 (m, 1H), 7.59 (s, 1H), 7.67 (d,  $J = 6.8$  Hz, 1H), 10.32 (br, 1H). HRMS:  $m/z$  (ES<sup>+</sup>) 459.1787 (MH<sup>+</sup>) for C<sub>21</sub>H<sub>26</sub>N<sub>6</sub>O<sub>4</sub>S.

**1-[6-(1-(2-(Dimethylamino)ethyl)-6-methyl-2-oxo-1,2-dihydropyridin-4-yl)-5-((tetrahydrofuran-3-yl)methoxy)thiazolo[5,4-b]pyridin-2-yl]-3-ethylurea (45).** Yield: 30%. <sup>1</sup>H NMR (300 MHz, DMSO-*d*<sub>6</sub>)  $\delta$  1.10 (t,  $J = 7.1$  Hz, 3H), 1.61–1.79 (m, 1H), 1.91–2.09 (m, 1H), 2.24 (s, 6H), 2.46 (s, 3H), 2.59–2.76 (m, 1H), 3.11–3.30 (m, 4H), 3.48–3.58 (m, 1H), 3.60–3.84 (m, 3H), 4.07 (t,  $J = 7.0$  Hz, 2H), 4.20–4.31 (m, 1H), 4.31–4.43 (m, 1H), 6.40 (s, 1H), 6.50 (s, 1H), 6.70 (t,  $J = 5.2$  Hz, 1H), 7.99 (s, 1H), 10.72 (br, 1H). HRMS:  $m/z$  (ES<sup>+</sup>) 501.2288 (MH<sup>+</sup>) for C<sub>24</sub>H<sub>32</sub>N<sub>6</sub>O<sub>4</sub>S.

**1-Ethyl-3-[6-(6-methyl-1-(2-morpholinoethyl)-2-oxo-1,2-dihydropyridin-4-yl)-5-((tetrahydrofuran-3-yl)methoxy)thiazolo[5,4-b]pyridin-2-yl]urea (46).** Yield: 30%. <sup>1</sup>H NMR (400 MHz, DMSO-*d*<sub>6</sub>)  $\delta$  1.09 (t,  $J = 7.3$  Hz, 3H), 1.65–1.76 (m, 1H), 1.98–2.08 (m, 1H), 2.47 (s, 3H), 2.53–2.59 (m, 4H), 2.61–2.72 (m, 1H), 3.13–3.25 (m, 2H), 3.31–3.345 (m, 2H), 3.51–3.70 (m, 6H), 3.72–3.82 (m, 2H), 4.09 (t,  $J = 6.8$  Hz, 2H), 4.25 (dd,  $J = 10.3, 7.8$  Hz, 1H), 4.36 (dd,  $J = 10.5, 6.5$  Hz, 1H), 6.42 (s, 1H), 6.51 (s, 1H), 6.69 (br, 1H), 8.00 (s, 1H), 10.78 (br, 1H). HRMS:  $m/z$  (ES<sup>+</sup>) 543.2408 (MH<sup>+</sup>) for C<sub>26</sub>H<sub>34</sub>N<sub>6</sub>O<sub>5</sub>S.

**Msm GyrB ATPase Assay.** The assay was carried out as described.<sup>17,22</sup> Briefly, GyrB ATPase assays were performed in 384-well Corning flat-bottomed plates in a 30  $\mu$ L reaction volume for 100 min at 25 °C with ATP at  $K_m$ . The hydrolysis of ATP was monitored by colorimetric estimation of the P<sub>i</sub> released.

**Determining the Antimycobacterial Properties of Thiazolopyridines.** *M. tuberculosis* H37Rv ATCC 27294 was used for the studies included in this work and grown as reported.<sup>25</sup> The minimum inhibitory concentration (MIC) was determined as described.<sup>17,22</sup>

**Killing Kinetics in 7H9 Broth.** This assay was performed in a 200  $\mu$ L volume using 96-well plates with Middlebrook 7H9 broth supplemented with 0.2% glycerol, 0.05% Tween 80 (Sigma), and 10% albumin dextrose catalase (Difco Laboratories). Serial 2-fold dilutions of thiazolopyridines covering a wide concentration range were added to each of the 96-wells containing approximately  $3 \times 10^7$  CFU/mL of Mtb H37Rv. The plates were incubated at 37 °C. Bacterial enumeration was performed on Middlebrook 7H11 agar plates at 0, 3, 7, and 14 days post drug treatment. The plates were incubated for 21–28 days at 37 °C in 5% CO<sub>2</sub> in a humidified atmosphere. The bacterial colonies were enumerated, and the data was expressed as the log<sub>10</sub>CFU for each drug concentration.

**Determination of Resistance Frequency.** Spontaneous resistant mutants were raised against compound 20 using a single-step selection method as described.<sup>17</sup> Briefly, a midlogarithmic phase culture of Mtb H37Rv was centrifuged and concentrated 100-fold to achieve a bacterial number of  $\sim 10^{10}$  CFU/mL. Varying dilutions of the bacterial culture were plated onto 20-containing plates (2–16  $\mu$ g/mL, corresponding to 8 $\times$ , 16 $\times$ , 32 $\times$ , and 64 $\times$  MIC concentrations of compound 20). For comparison, bacteria were plated on rifampicin containing plates (0.24 and 0.48  $\mu$ g/mL, corresponding to 8 $\times$  and 16 $\times$  MIC concentration of rifampicin, respectively). Appropriate dilutions of the bacterial culture were also plated on drug-free Middlebrook 7H11 agar to enumerate the bacterial numbers in the culture. Plates were incubated for 4 weeks at 37 °C, and the CFUs in the drug-free plates were enumerated. The drug-containing plates were incubated for up to 6–8 weeks at 37 °C to confirm the final number of spontaneously resistant colonies.

The spontaneous rate of resistance was calculated by dividing the number of colonies on drug-containing plates (at a given concentration) divided by the total number of viable bacteria



estimated on drug-free plates. Resistant colonies were randomly picked from the drug containing plates and grown in complete 7H9 broth to determine their level of resistance against compound **20** as well as other standard TB drugs with different mechanisms of action.

**Genetic Mapping of Mutations Conferring Resistance to Thiazolopyridine Ureas.** To determine the genetic basis for resistance to thiazolopyridines, the *gyrB* gene of the spontaneous resistant mutants was sequenced. Chromosomal DNA was isolated from well-characterized resistant clones by boiling the cultures for 20 min. The boiled supernatants were subjected to PCR analysis using specific Mtb *gyrB* primers to amplify the entire *gyrB* gene (forward 5'-GACGCACGGCGCGGTTAGA-3' and reverse 5'-TTAGACATCC-AGGAACCGAA-3'). PCR was performed with cycling parameters of 94 °C for 30 s, 67.5 °C for 30 s, and 72 °C for 2 min for 30 cycles in a DNA Engine Dyad cycler (Bio-Rad). PCR products were cleaned (PCR purification kit, Qiagen), quantitated, and sequenced (Micro-synth). The sequences from the resistant clones were aligned against the wild-type H37Rv *gyrB* gene using Vector NTI software to detect mutations in the target gene.

**In Vivo Efficacy in a Murine Model of TB.** All animal experiments were approved by the Institutional Animal Ethics Committee (IAEC). Balb/c mice were infected with Mtb H37Rv through the aerosol route as described, resulting in an installation of ~10 000 CFU/lung.<sup>25</sup> Isoniazid at 3 mg/kg was used as a reference drug in a formulation containing 0.5% w/v hydroxypropyl methyl cellulose (HPMC), whereas compound **23** was prepared in 0.5% w/v of HPMC and 0.1% w/v Tween, as for the PK study.

Infected mice were treated with an oral dose of 100 mg/kg once daily, 150 mg/kg twice daily, or 300 mg/kg once daily of compound **23** for 10 days of continuous dosing. Treatment commenced 3 days postinfection. At the end of 10 doses, mice were sacrificed, and appropriate dilutions of the lung homogenates were plated on Middlebrook 7H11 agar plates to determine viable CFU per lung. Three mice were used for each of the vehicle- or compound-treated groups. A group of three mice was sacrificed at the start of treatment to serve as early controls.

## ■ ASSOCIATED CONTENT

### ● Supporting Information

Primary sequence alignment of Msm, Mtb GyrB, and Spn ParE; crystallography materials and methods; docked poses of compounds **21** and **25** in the Spn ParE crystal structure; synthetic procedures for the intermediates. This material is available free of charge via the Internet at <http://pubs.acs.org>.

## ■ AUTHOR INFORMATION

### Corresponding Author

\*Phone: +91 80 23621212 ext 6274. Fax: +91 80 23621214. E-mail: [sandeep.ghorpade@astrazeneca.com](mailto:sandeep.ghorpade@astrazeneca.com).

### Present Addresses

○Medicines for Malaria Venture (MMV), Switzerland.

◆Novartis Institute for Tropical Diseases, Singapore.

¶Quintiles, Bangalore, India.

■C-CAMP, Bangalore, India.

★Vipragen, Mysore, India.

⊞Northern Institute of Cancer Research, University of Newcastle, Newcastle-upon-Tyne, United Kingdom.

△Epizyme, Cambridge, Massachusetts, United States.

### Author Contributions

▽These authors contributed equally.

### Notes

The authors declare no competing financial interest.

## ■ ACKNOWLEDGMENTS

We thank Sreenivasiah Menasinakai and Sandesh Jatheen-dranath for purification and analytical support, including NMR

studies, as well as the compound management group at AstraZeneca for all compound dispensing and dispatch-related activities. We thank Guo Chen and D. Bryan Prince for their contributions to the preparation of the Spn ParE protein for crystallization.

## ■ ABBREVIATIONS USED

TB, tuberculosis; Mtb, *Mycobacterium tuberculosis*; Msm, *Mycobacterium smegmatis*; MIC, minimum inhibitory concentration; HB, H bond; SAR, structure–activity relationship; AUC, area under the curve; f, free fraction; QD, once a day; BID, twice a day; CFU, colony forming units; rt, room temperature; DME, 1,2-dimethoxyethane; THF, tetrahydrofuran; DMF, *N,N*-dimethylformamide; DEAD, diethyl azodicarboxylate; DIAD, diisopropyl azodicarboxylate

## ■ REFERENCES

- (1) World Health Organization. *Global Tuberculosis Control*; WHO 2011 Report on Tuberculosis. [http://www.who.int/mediacentre/news/releases/2011/tb\\_2011011/en/index.html](http://www.who.int/mediacentre/news/releases/2011/tb_2011011/en/index.html)
- (2) World Health Organization. *Multidrug and Extensively Drug-Resistant TB (M/XDR-TB)*; WHO 2010 Global Report on Surveillance and Response.
- (3) Wong, E. B.; Cohen, K. A.; Bishai, W. R. Rising to the challenge: New therapies for tuberculosis. *Trends Microbiol.* **2013**, *21*, 493–501.
- (4) Skripconoka, V.; Danilovits, M.; Pehme, L.; Tomson, T.; Skenders, G.; Kummik, T.; Cirule, A.; Leimane, V.; Kurve, A.; Levina, K.; Geiter, L. J.; Manissero, D.; Wells, C. D. Delamanid improves outcomes and reduces mortality in multidrug-resistant tuberculosis. *Eur. Respir. J.* **2013**, *41*, 1393–1400.
- (5) Sacksteder, K. A.; Protopopova, M.; Barry, C. E., 3rd; Andries, K.; Nacy, C. A. Discovery and development of SQ109: A new antitubercular drug with a novel mechanism of action. *Future Microbiol.* **2012**, *7*, 823–837.
- (6) Leach, K. L.; Brickner, S. J.; Noe, M. C.; Miller, P. F. Linezolid, the first oxazolidinone antibacterial agent. *Ann. N.Y. Acad. Sci.* **2011**, *1222*, 49–54.
- (7) Migliori, G. B.; Langendam, M. W.; D'Ambrosio, L.; Centis, R.; Blasi, F.; Huitric, E.; Manissero, D.; van der Werf, M. J. Protecting the tuberculosis drug pipeline: stating the case for the rational use of fluoroquinolones. *Eur. Respir. J.* **2012**, *40*, 814–822.
- (8) Zumla, A.; Nahid, P.; Cole, S. T. Advances in the development of new tuberculosis drugs and treatment regimens. *Nat. Rev. Drug Discovery* **2013**, *12*, 388–404.
- (9) (a) Burman, W. J.; Goldberg, S.; Johnson, J. L.; Muzanye, G.; Engle, M.; Mosher, A. W.; Choudhary, S.; Daley, C. L.; Munsiff, S. S.; Zhao, Z.; Vernon, A.; Chaisson, R. E. Moxifloxacin versus ethambutol in the first 2 months of treatment for pulmonary tuberculosis. *Am. J. Respir. Crit. Care Med.* **2006**, *174*, 331–338. (b) Conde, M. B.; Efron, A.; Lored, C.; De Souza, G. R.; Graca, N. P.; Cezar, M. C.; Ram, M.; Chaudhary, M. A.; Bishai, W. R.; Kritski, A. L.; Chaisson, R. E. Moxifloxacin in the initial therapy of tuberculosis: A randomized, phase 2 trial. *Lancet* **2009**, *373*, 1183–1189. (c) Duong, D. A.; Nguyen, T. H.; Nguyen, T. N.; Dai, V. H.; Dang, T. M.; Vo, S. K.; Do, D. A.; Nguyen, V. V.; Nguyen, H. D.; Dinh, N. S.; Farrar, J.; Caws, M. Beijing genotype of *Mycobacterium tuberculosis* is significantly associated with high-level fluoroquinolone resistance in Vietnam. *Antimicrob. Agents Chemother.* **2009**, *53*, 4835–4839.
- (10) Cole, S. T.; Brosch, R.; Parkhill, J.; Garnier, T.; Churcher, C.; Harris, D.; Gordon, S. V.; Eiglmeier, K.; Gas, S.; Barry, C. E., III; Tekaia, F.; Badcock, K.; Basham, D.; Brown, D.; Chillingworth, T.; Connor, R.; Davies, R.; Devlin, K.; Feltwell, T.; Gentles, S.; Hamlin, N.; Holroyd, S.; Hornsby, T.; Jagels, K.; Krogh, A.; McLean, J.; Moule, S.; Murphy, L.; Oliver, K.; Osborne, J.; Quail, M. A.; Rajandream, M.-A.; Rogers, J.; Rutter, S.; Seeger, K.; Skelton, J.; Squares, R.; Squares, S.; Sulston, J. E.; Taylor, K.; Whitehead, S.; Barrell, B. G. Deciphering

the biology of *Mycobacterium tuberculosis* from the complete genome sequence. *Nature* **1998**, 393, 537–544.

(11) Blattner, F. R.; Plunkett, G., III; Bloch, C. A.; Perna, N. T.; Burland, V.; Riley, M.; Collado-Vides, J.; Glasner, J. D.; Rode, C. K.; Mayhew, G. F.; Gregor, J.; Wayne Davis, N.; Kirkpatrick, H. A.; Goeden, M. A.; Rose, D. J.; Mau, B.; Shao, Y. The complete genome sequence of *Escherichia coli* K-12. *Science* **1997**, 277, 1453–1462.

(12) Drlica, K.; Malik, M.; Kerns, R. J.; Zhao, X. Quinolone-mediated bacterial death. *Antimicrob. Agents Chemother.* **2008**, 52, 385–392.

(13) Lewis, I. J.; Singh, O. M. P.; Smith, C. V.; Skarzynski, T.; Maxwell, A.; Wonacott, A. J.; Wigley, D. B. The nature of inhibition of DNA gyrase by the coumarins and the cyclothialidines revealed by X-ray crystallography. *EMBO J.* **1996**, 15, 1412–1420.

(14) Shirude, P. S.; Hameed, S. Nonfluoroquinolone-based inhibitors of mycobacterial type II topoisomerase as potential therapeutic agents for TB. In *Annual Reports in Medicinal Chemistry*; Desai, M. C., Ed.; Academic Press: Burlington, MA, 2012; Vol. 47, pp 319–330.

(15) (a) Chopra, S.; Matsuyama, K.; Tran, T.; Malerich, J. P.; Wan, B.; Franzblau, S. G.; Lun, S.; Guo, H.; Maiga, M. C.; Bishai, W. R.; Madrid, P. B. Evaluation of gyrase B as a drug target in *Mycobacterium tuberculosis*. *J. Antimicrob. Chemother.* **2012**, 67, 415–421. (b) Charifson, P. S.; Grillot, A.-L.; Grossman, T. H.; Parsons, J. D.; Badia, M.; Bellon, S.; Deininger, D. D.; Drumm, J. E.; Gross, C. H.; LeTiran, A.; Liao, Y.; Mani, N.; Nicolau, D. P.; Perola, E.; Ronkin, S.; Shannon, D.; Swenson, L. L.; Tang, Q.; Tessier, P. R.; Tian, S.-K.; Trudeau, M.; Wang, T.; Wei, Y.; Zhang, H.; Stamos, D. Novel dual-targeting benzimidazole urea inhibitors of DNA gyrase and topoisomerase IV possessing potent antibacterial activity: Intelligent design and evolution through the judicious use of structure-guided design and structure-activity relationships. *J. Med. Chem.* **2008**, 51, 5243–5263. (c) Grossman, T. H.; Bartels, D. J.; Mullin, S.; Gross, C. H.; Parsons, J. D.; Liao, Y.; Grillot, A.; Stamos, D.; Olson, E. R.; Charifson, P. S.; Mani, N. Dual targeting of GyrB and ParE by a novel amino-benzimidazole class of antibacterial compounds. *Antimicrob. Agents Chemother.* **2007**, 51, 657–666.

(16) Shahul, P. H.; Waterson, D. 2-(Piperin-1-yl)-4-azolyl-thiazole-5-carboxylic acid derivatives against bacterial infections. *PCT International Patent* WO2010067125, 2010.

(17) Shirude, P. S.; Madhavapeddi, P.; Tucker, J. A.; Murugan, K.; Patil, V.; Basavarajappa, H.; Raichurkar, A. V.; Humnabadkar, V.; Hussein, S.; Sharma, S.; Ramya, V. K.; Narayan, C. B.; Balganes, T. S.; Sambandamurthy, V. K. Aminopyrazinamides: Novel and specific GyrB inhibitors that kill replicating and nonreplicating *Mycobacterium tuberculosis*. *ACS Chem. Biol.* **2013**, 8, 519–523.

(18) East, S. P.; White, C. B.; Barker, O.; Barker, S.; Bennett, J.; Brown, D.; Boyd, E. A.; Brennan, C.; Chowdhury, C.; Collins, I.; Convers-Reignier, E.; Dymock, B. W.; Fletcher, R.; Haydon, D. J.; Gardiner, M.; Hatcher, S.; Ingram, P.; Lancett, P.; Mortenson, P.; Papadopoulos, K.; Smees, C.; Thomaidis-Brears, H. B.; Tye, H.; Workman, J.; Czaplewski, L. G. DNA gyrase (GyrB)/topoisomerase IV (ParE) inhibitors: Synthesis and antibacterial activity. *Bioorg. Med. Chem. Lett.* **2009**, 19, 894–899.

(19) (a) Haydon, D. R.; Czaplewski, L. G.; Palmer, N. J.; Mitchell, D. R.; Atherall, J. F.; Steele, C. R.; Ladduwahetty, T. Antibacterial compositions. *PCT International Patent* WO2007148093, 2007. (b) Haydon, D. J.; Czaplewski, L. G. Antibacterial condensed thiazoles. *PCT International Patent* WO2009074812, 2009.

(20) Starr, J. T.; Sciotti, R. J.; Hanna, D. L.; Huband, M. D.; Mullins, L. M.; Cai, H.; Gage, J. W.; Lockard, M.; Rauckhorst, M. R.; Owen, R. M.; Lall, M. S.; Tomilo, M.; Chen, H.; McCurdy, S. P.; Barbachyn, M. R. 5-(2-Pyrimidinyl)-imidazo[1,2-a]pyridines are antibacterial agents targeting the ATPase domains of DNA gyrase and topoisomerase IV. *Bioorg. Med. Chem. Lett.* **2009**, 19, 5302–5306.

(21) (a) Sherer, B.; Zhou, F. Heterocyclic urea derivatives and methods of use thereof. *PCT International Patent* WO2009147440, 2009. (b) Hill, P.; Manchester, J. I.; Sherer, B.; Choy, A. L. Heterocyclic urea derivatives for the treatment of bacterial infections. *PCT International Patent* WO2009147433, 2009.

(22) Ghorpade, S. R.; Kale, M. G.; McKinney, D. C.; Shahul, P. H.; Raichurkar, A. K. Thiazolo[5, 4-b]pyridine and oxazolo[5, 4-b]pyridine derivatives as antibacterial. *PCT International Patent* WO2009147431, 2009.

(23) Homology model: The Mtb-GyrB structure was built by homology modelling using the SwissModel (<http://swissmodel.expasy.org/>) automated web server. The published *E.coli*-GyrB (PDB ID: 1EI1A, 2.3 Å) structure was used as a template for model building. After aligning the generated model onto the reference template, the ligand and the conserved water molecule of the reference template were extracted and merged with the Mtb-GyrB model in VIDA (version 4.0.3, OpenEye Sci. Software). The resultant binary complex model was further analyzed in Maestro (version 8; Schrödinger, LLC) using the default parameters of the Protein Preparation Tool and subjected subsequently to an energy minimization of 5000 steps. The energy-minimized model was used for further studies.

(24) (a) Haihong, N.; Wendoloski, J. Structure-based design of new antibacterial agents. *Ann. Rep. Comput. Chem.* **2006**, 2, 279–295. (b) Sherer, B. A.; Hull, K.; Green, O.; Basarab, G.; Hauck, S.; Hill, P.; Loch, J. T., 3rd; Mullen, G.; Bist, S.; Bryant, J.; Boriack-Sjodin, A.; Read, J.; DeGrace, N.; Uria-Nickelsen, M.; Illingworth, R. N.; Eakin, A. E. Pyrrolamide DNA gyrase inhibitors: Optimization of antibacterial activity and efficacy. *Bioorg. Med. Chem. Lett.* **2011**, 21, 7416–7420.

(25) Jayaram, R.; Gaonkar, S.; Kaur, P.; Suresh, B. L.; Mahesh, B. N.; Jayashree, R.; Nandi, V.; Bharat, S.; Shandil, R. K.; Kantharaj, E.; Balasubramanian, V. Pharmacokinetics-pharmacodynamics of rifampin in an aerosol infection model of tuberculosis. *Antimicrob. Agents Chemother.* **2003**, 47, 2118–2124.